Image Cover Sheet

CA011310

CLASSIFICATION	SYSTEM NUMBER 515888
UNCLASSIFIED	

TITLE

Aerodynamic characteristics of the BDU-5003/B MOD 1 bomb at subsonic velocities from aeroballistic range free-flight tests

System Number:

Patron Number:

Requester:

Notes:

DSIS Use only:

Deliver to:

Report Documentation Page

Public reporting burden for the collection of information is estimated to average 1 hour per response, including the time for reviewing instructions, searching existing data sources, gathering and maintaining the data needed, and completing and reviewing the collection of information. Send comments regarding this burden estimate or any other aspect of this collection of information, including suggestions for reducing this burden, to Washington Headquarters Services, Directorate for Information Operations and Reports, 1215 Jefferson Davis Highway, Suite 1204, Arlington VA 22202-4302. Respondents should be aware that notwithstanding any other provision of law, no person shall be subject to a penalty for failing to comply with a collection of information if it does not display a currently valid OMB control number.

1. REPORT DATE **JUN 2000**	2. REPORT TYPE	3. DATES COVERED

4. TITLE AND SUBTITLE **Aerodynamic characteristics of the BDU-5003/B MOD 1 bomb at subsonic velocities from aeroballistic range free-flight tests**	5a. CONTRACT NUMBER
	5b. GRANT NUMBER
	5c. PROGRAM ELEMENT NUMBER
6. AUTHOR(S)	5d. PROJECT NUMBER
	5e. TASK NUMBER
	5f. WORK UNIT NUMBER
7. PERFORMING ORGANIZATION NAME(S) AND ADDRESS(ES) **Defence R&D Canada - Valcartier,2459 Pie-XI Blvd North,Quebec (Quebec) G3J 1X5 Canada, ,**	8. PERFORMING ORGANIZATION REPORT NUMBER
9. SPONSORING/MONITORING AGENCY NAME(S) AND ADDRESS(ES)	10. SPONSOR/MONITOR'S ACRONYM(S)
	11. SPONSOR/MONITOR'S REPORT NUMBER(S)

12. DISTRIBUTION/AVAILABILITY STATEMENT
Approved for public release; distribution unlimited.

13. SUPPLEMENTARY NOTES

14. ABSTRACT
Free-flight tests were conducted in the Defence Research Establishment Valcartier (DREV) aeroballistic range on a full-scale MPB-IID (BDU-5003/B MOD 1) bomb at subsonic velocities. All the main aerodynamic coefficients and dynamic stability derivatives were very well determined using the six-degree-of-freedom single- and multiple-fit data reduction techniques. The free-flight data shows that this bomb is dynamically unstable at low angles of attack. The second order pitch damping coefficient the yaw axial force term as well as side moments were also reduced. Wind tunnel, Open Jet Facility experimental results and full-scale aircraft free-flight trials were compared with the aeroballistic ones.

15. SUBJECT TERMS

16. SECURITY CLASSIFICATION OF:			17. LIMITATION OF ABSTRACT	18. NUMBER OF PAGES **72**	19a. NAME OF RESPONSIBLE PERSON
a. REPORT **unclassified**	b. ABSTRACT **unclassified**	c. THIS PAGE **unclassified**			

This page is left blank

This page is left blank

REPRODUCTION QUALITY NOTICE

This document is the best quality available. The copy furnished to DRDCIM contained pages that may have the following quality problems:

: Pages smaller or Larger than normal

: Pages with background colour or light coloured printing

: Pages with small type or poor printing; and or

: Pages with continuous tone material or colour photographs

Due to various output media available these conditions may or may not cause poor legibility in the hardcopy output you receive.

☒ If this block is checked, the copy furnished to DRDCIM contained pages with colour printing, that when reproduced in Black and White, may change detail of the original copy.

UNCLASSIFIED

DEFENCE RESEARCH ESTABLISHMENT
CENTRE DE RECHERCHES POUR LA DÉFENSE
VALCARTIER, QUÉBEC

DREV - TR – 2000-229
Unlimited Distribution / Distribution illimitée

AERODYNAMIC CHARACTERISTICS OF THE BDU-5003/B MOD 1

BOMB AT SUBSONIC VELOCITIES FROM
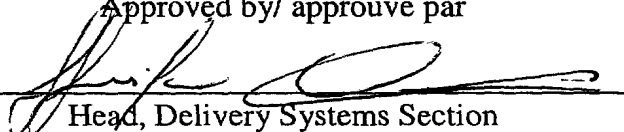
AEROBALLISTIC RANGE FREE-FLIGHT TESTS

by

A. D. Dupuis and Wayne Hathaway*

June/juin 2001

*Arrow Tech Associates

Approved by/ approuvé par

_____
Head, Delivery Systems Section
Chef, Section systèmes de lancement

_____
17 June 2001
Date

SANS CLASSIFICATION

WARNING NOTICE

ABSTRACT

Free-flight tests were conducted in the Defence Research Establishment Valcartier (DREV) aeroballistic range on a full-scale MPB-HD (BDU-5003/B MOD 1) bomb at subsonic velocities. All the main aerodynamic coefficients and dynamic stability derivatives were very well determined using the six-degree-of-freedom single- and multiple-fit data reduction techniques. The free-flight data shows that this bomb is dynamically unstable at low angles of attack. The second order pitch damping coefficient, the yaw axial force term as well as side moments were also reduced. Wind tunnel, Open Jet Facility experimental results and full-scale aircraft free-flight trials were compared with the aeroballistic ones.

RÉSUMÉ

Des essais en vol libre ont été effectués dans le corridor aérobalistique du Centre de recherches pour la défense Valcartier (CRDV) avec la bombe pleine échelle MPB-HD (BDU-5003/B MOD 1) aux vitesses subsoniques. Tous les coefficients aérodynamiques principaux et les dérivés de stabilité dynamique ont été très bien déterminés avec les méthodologies de réduction de six degrés de liberté par les options de réduction simple et multiple. Les données en vol libre démontrent que cette bombe est dynamiquement instable à faible angle d'incidence. Le deuxième terme du coefficient d'amortissement de tangage, le terme du deuxième ordre pour la force axiale ainsi que les moments de côté ont aussi été réduits. Les résultats expérimentaux de la soufflerie à rafale et à jet libre ainsi que des essais d'aéronefs sont comparés à ceux obtenus dans le corridor aérobalistique.

TABLES OF CONTENTS

UNCLASSIFIED

v

EXECUTIVE SUMMARY

The CF have developed a Store Separation Model (SSM) to predict the separation of stores from the CF-18 aircraft given a configuration and initial conditions. This model was developed in order to reduce the risks of flight test incidents, and to reduce store separation work by directing efforts to critical areas. SSM has been used extensively by Canadair on behalf of DND to support various CF-18 stores clearance projects in the past. The current flight matching technique uses a trial and error approach, which is very time-consuming and costly. It was shown recently that the implementation of the Maximum Likelihood Method (MLM) in the SSM could resolve its inherent deficiencies. The MLM has the capability of extracting aerodynamic coefficients and interference parameters, simultaneously from measured store separation trajectories. The Ballistic SSM (BSSM), under development, would be able to predict full-scale separation and ballistic flight test data for the CF-18 aircraft.

Even though the MLM is a well-proven technique to extract interference coefficients and aerodynamic coefficients (static and dynamic), the store separation tests usually do not have enough angular and translational motion so that it can be utilized to its maximum efficiency. It is therefore required to have a very good free stream aerodynamic (static and dynamic) coefficient database of stores dropped from the CF-18 to be able to extract the interference coefficients with a high degree of confidence. If the free stream aerodynamics of the store are in error, the MLM will over- or underestimate the interference coefficients to fit the overall observed motion. This reliable free stream aerodynamic database will also be used with the BSSM and the DREV 6DOF trajectory simulation program to predict accurate store impact at the target and in the CF-18 Ballistic Integrator Algorithm OFP.

DREV has a unique free - flight aeroballistic range where aerodynamic coefficients (static and dynamic) are reduced from measured trajectories with the MLM methodology. Projectiles (scaled or full scale) are fired from a powder gun through 54 indirect shadowgraph stations. This aeroballistic range has shown over the years to be able to extract very reliable aerodynamic coefficients.

DREV was tasked by NDHQ to fire a first series of store configurations in the DREV aeroballistic range with the goal of obtaining their free stream static and dynamic aerodynamic coefficients. A second objective was to evaluate various available tools to predict the aerodynamic coefficients in view of reducing costs of experimental tests. The stores that were chosen for this first phase were: LDGP MK82 CF, BDU-5002/B Mod 1 (Modular Practice Bomb - Low Drag), and BDU-5003/B MOD 1 (Modular Practice Bomb - High Drag). The Mach number range of interest is between Mach 0.6 and 1.5.

This report presents the aerodynamic coefficients and stability derivatives that were deduced from free-flight tests conducted in the DREV aeroballistic range on a full-

vi

scale BDU-5003/B Mod 1 (Modular Practice Bomb - High Drag) bomb. All the main aerodynamic coefficients and dynamic stability derivatives as well as nonlinear ones were determined using the six-degree-of-freedom single- and multiple-fit data reduction techniques. The measured angular motion of all the shots fired in the aeroballistic range shows a growth as the projectile flies downrange. This indicates that this bomb is dynamically unstable at low angles of attack. The second order pitch damping coefficient, the yaw axial force term as well as side moments were also reduced. Wind tunnel, Open Jet Facility experimental results as well as full scale free-trials were compared with the aeroballistic range ones.

The data from these trials combined with the ones from the DREV Open Jet Facility suggests that this bomb flies with a limit cycle of approximately 8.0° and 12.0° angle of attack.

This database of aerodynamic coefficients generated by this experimental program is considered a success and it can be used with the BSSM, the SSM as well as the DREV 6DOF trajectory program to predict accurate weapon performance. Also, it can be exploited with confidence for the CF-18 OFP. The methodology should be expanded to other weapon systems.

NOMENCLATURE

Variable	Computer Output	Description
A		Cross sectional area of projectile (m^2)
d		Diameter of projectile (mm)
c. g.	CG	Center of gravity (m)
C_{l_p}		Roll damping moment coefficient
$C_{l\delta}$		Roll moment coefficient due to fin cant
$C_{l\gamma}$	Clg	Induced roll moment coefficient
C_{np}	Cnp	Magnus moment coefficient
$C_{n\gamma}$	Cng	Induced yaw moment coefficient
C_{nsm}	Cnsm	Side moment coefficient
C_N	CN	Normal force coefficient
$C_{N_\delta}\delta_A$	CNda	Trim force coefficient component
$C_{N_\delta}\delta_B$	CNdB	Trim force coefficient component
C_M	Cm	Static pitch moment coefficient
C_{Mq}	Cmq	Pitch damping moment coefficient
$C_{M_\delta}\delta_A$	Cmda	Trim moment coefficient component
$C_{M_\delta}\delta_B$	CmdB	Trim moment coefficient component
$C_{m\gamma}$	Cmg	Induced pitching moment coefficient
C_{X0}	CX0	Axial force coefficient at zero angle of attack
C_{Yp}	CYp	Magnus moment coefficient
$C_{Y\gamma}$	CYg	Induced normal force coefficient
$C_{Z\gamma}$	CZg	Induced normal force coefficient

I_x, I_y	-	Axial and transverse moments of inertia (kg m^2)
l	-	Length of projectile (m)
l/d	-	Length-to-diameter ratio
m	-	Mass of projectile (kg)
M	Mach	Mach number
MPB-HD	-	Modular Practice Bomb - High Drag
p	-	Spin rate (rad/s or deg/m)
Re_l	-	Reynolds number based on length of projectile
u, v, w	-	Projectile component velocities (m/s)
V	-	Total projectile velocity (m/s)
X, Y, Z	-	Projectile coordinates (m)
t	-	Time of flight (s)
$\bar{\alpha}$	a	Total angle of attack (deg)
$\bar{\alpha}_{max}$	AMAX	Maximum angle of attack (deg)
λ_N, λ_P	LN, LP	Nutation and precession damping (1/m)
θ, ψ, ϕ	-	Projectile orientation (deg)
δ	-	Fin cant angle (rad or deg)
δ_T	-	Total trim angle (rad or deg)
$\bar{\delta}^2$	DBSQ	Mean squared yaw (deg^2)
ε	-	Sine of the total angle of attack, $$\sin\bar{\alpha} = \frac{v^2 + w^2}{V^2}$$
ρ	-	Air density (kg/m^3)
6DOF	-	Six degree of freedom

UNCLASSIFIED

ix

Subscripts

| $\overline{\alpha}_i$ | ai (i) | Derivative with respect to ε_i |
| M | M | Variation with Mach number |

Examples

$C_{M\overline{\alpha}}$	Cma	Pitching moment coefficient slope
$C_{M\overline{\alpha}3}$	Cma3	Pitching moment coefficient w.r.t. ε^3
$C_{Mq\overline{\alpha}2}$	Cmq2	Pitch damping coefficient w.r.t. ε^2

UNCLASSIFIED

UNCLASSIFIED

1

1.0 <u>INTRODUCTION</u>

The CF has developed a Store Separation Model (SSM) to predict the separation of stores from the CF-18 aircraft given a configuration and initial conditions in order to reduce the risks of flight test incidents, and to reduce store separation work by directing efforts to critical areas. SSM has been used extensively by Canadair on behalf of DND to support various CF-18 stores clearance projects in the past. Because of inherent model limitations, it is essential to implement the capability to adjust aerodynamic coefficients from the SSM database to match model predictions with flight test data. The current flight matching technique uses an ineffective trial and error approach, which is very time-consuming and costly.

The Defense Research Establishment Valcartier (DREV) has successfully implemented a computerized system which uses the Maximum Likelihood Method (MLM) to iteratively extract aerodynamic coefficients and interference parameters, simultaneously, from the trajectory of test articles in their aeroballistic range and Open Jet Facility. The heart of this system are two computer programs known as the Aeroballistic Range Facility Data Analysis System (ARFDAS, Ref. 1) and Open Jet Facility Data Analysis System (OJFDAS, Ref. 2). OJFDAS, (Ref. 2), successfully showed that it was possible to extract store separation interference coefficients and free stream aerodynamic coefficients (static and dynamic), simultaneously. Feasibility work, which confirmed the compatibility of the MLM algorithms with the SSM, was carried out under MLM Phase 1 efforts (Ref. 3).

A SSM and Ballistic Store Separation Model (BSSM) compatible MLM algorithm, known as the Store Separation Model Data Analysis System (SSMDAS), was tested, under Phase 1 (Ref. 3) efforts and confirmed the ability of MLM techniques to correctly adjust aerodynamic free stream and interference coefficients to match SSM/BSSM predictions to full-scale separation and ballistic flight test data for the CF-18 aircraft. Implementation of such an automated system will improve the accuracy and efficiency of

DND's SSM and BSSM for future store separation and ballistics work. Canadair has implemented the MLM in the SSM and BSSM (Ref. 4). The modified SSM and BSSM shall have the capability of using MLM techniques to achieve a match of SSM/BSSM predicted trajectories to actual observed separation and free-flight trajectory data of stores dropped from CF-18 aircraft during flight test.

Even though the MLM is a well-proven technique to extract interference coefficients and aerodynamic coefficients (static and dynamic), the store separation tests usually do not have enough angular and translational motion so that it can be utilized to its maximum efficiency. It is therefore required to have a very good free stream aerodynamic (static and dynamic) coefficient database of stores dropped from the CF-18 to be able to extract the interference coefficients with a high degree of confidence. If the free stream aerodynamics of the store are in error, the MLM will overcompensate for this, which might lead to errors in the determined interference coefficients. This reliable free stream aerodynamic database will also be used with the BSSM to predict accurate store impact at the target and in the CF-18 Ballistic Integrator Algorithm OFP. An NRC report (Ref. 5) also states this requirement for a reliable aerodynamic database: "In this component approach to store integration, the essential baseline information is the store free stream aerodynamics. The aircraft flow field, carriage loads, and launch characteristics are considered as interferences (not necessarily small) to the aerodynamic characteristic of the store. Hence, whether flight tests, ground tests, or computations are used, a well-established aerodynamic database for the store itself should be obtained".

DREV has a unique free-flight aeroballistic range (Ref. 6 and 7) where absolute aerodynamic coefficients (static and dynamic) are readily obtainable from measured trajectories with the MLM methodology. Scaled or full-scale projectiles can be fired from a powder gun through 54 indirect shadowgraph stations. This aeroballistic range has shown over the years to be able to extract very reliable aerodynamic coefficients.

UNCLASSIFIED
3

DREV was tasked by NDHQ to fire a first series of store configurations in the DREV aeroballistic range with the goal of obtaining their free stream static and dynamic aerodynamic coefficients. A second objective was to evaluate various available tools to predict the aerodynamic coefficients in view of reducing the costs of experimental testing. The stores that were chosen for this first phase were: a scaled LDGP MK-82 CF (18.6%), a full-scale BDU-5002/B Mod 1 (Modular Practice Bomb - Low Drag, MPB-LD) and the BDU-5003/B Mod 1 (Modular Practice Bomb - High Drag, MPB - HD). The Mach number range of interest is between Mach 0.6 and 1.5.

This report presents the aerodynamic coefficients and stability derivatives that were deduced from free-flight trajectories measured in the DREV aeroballistic range on a full-scale BDU-5003/B Mod 1 (Modular Practice Bomb - High Drag) bomb. All the main aerodynamic coefficients and dynamic stability derivatives as well as nonlinear ones were determined using the six-degree-of-freedom single- and multiple-fit data reduction techniques. The measured angular motion of all the shots fired in the aeroballistic range shows a growth in the incidence as the projectile flies downrange. This indicates that this bomb is dynamically unstable at low angles of attack. The second order pitch damping coefficient, the yaw axial force term as well as side moments were also reduced. Wind tunnel, Open Jet Facility experimental results as well as full-scale free-trials were compared with the aeroballistic range ones.

This trial was performed at DREV in October 1998 and the analysis in February 1999, under Work Unit 3ec16, Improvement to CF-18 Ballistics Algorithms.

UNCLASSIFIED
4

2.0 MODEL CONFIGURATION

2.1 MPB-HD Configuration

The full-scale MPB-HD was a proper candidate since its caliber (50.8 mm) was a suitable size to fire in the DREV aeroballistic range at full scale. Also, an extensive wind tunnel database exists at DREV with this configuration and it was also tested at length from aircraft. This was also one of the configurations that were tested in the DREV Open Jet Facility and used as a basis to validate the MLM methodology in obtaining store interference coefficients and free stream aerodynamic coefficients, simultaneously (Ref. 2).

The in-service MPB-HD configuration was used. The main dimensions are provided in Fig. 1 in caliber. The reference diameter is 50.8 mm. The only external geometry difference from the standard practice bomb is that the fins were rotated 45° from the locator holes, i.e. one pair of fins is in line with the locator holes. This was done so as to be able to launch them with the sabot that was designed (Ref. 8). The fumer cartridge was also replaced by a dummy one to keep the center of gravity and the mass as close as possible to the in service bomb.

The MPB-HD has a 1.35 cal ogive nose followed by a 4.07 cal cylindrical portion and the fins are placed at the end of an 2.48 cal extended boattail. The fins have a 2.00 cal span and are of a clipped delta type. The fin leading edges are blunt with a thickness of 0.08 cal which reduces to 0.05 cal at the trailing edge. The MPB-HD has the same fin and body dimensions as the LD version. A high drag 0.07 cal thick retardation disk with a diameter of 1.76 cal is located at 1.89 cal from the nose. A 1.7 cal diameter high drag conical tail is placed just aft of the fins. The fin type and main dimensions are the same as in the low drag version. The fins have no cant to produce spin rate. The center of gravity of the tested projectiles was located at 3.97 caliber from the nose with the dummy cartridge in the projectile. The total length of the projectile is 8.55 cal.

The nominal physical properties of the model are given in Table I and the physical properties of each test projectile are provided in Table II.

2.2 Sabot Design

Since the projectile had to be launched from a powder gun to conduct tests in the DREV aeroballistic range, special sabots had to be designed to fire them. Since the model configuration in this case is fin stabilized, a smooth bore gun was utilized. The standard gun employed at DREV to fire fin-stabilized projectiles of these dimensions in the aeroballistic range is a 110-mm smooth bore gun.

Several aspects have to be considered when designing sabots and models. They are: projectile configuration, total mass, sabot separation at the sabot trap located at 9.2 m from the muzzle at the aeroballistic range, muzzle velocity desired, gun accelerations, etc. The last three mentioned have to be consistent from round to round. In these tests, the highest muzzle velocity achieved was approximately 323 m/s (Mach 0.95) and the lowest, 270 m/s (Mach 0.8).

The tail portion of the modular practice bombs is made of a polycarbonate material. Therefore, it is impossible to launch them with a base plate pusher sabot since the projectile would disintegrate at launch. The modular practice bombs have two locator holes situated close to the center of gravity (Ref.8) and a sabot design that would pull the projectile by these holes presented an interesting option.

Figure 2 shows a schematic of the sabot with the MPB-HD projectile inside it. The sabot for the MPB-LD is exactly the same. The detail drawings of the sabot are provided in Ref. 8. It is a two petal sabot design made of aluminum. The lengths of the saw cuts on each side were adjusted to obtain adequate petal separation for the expected velocities. A

sabot base seal pad was also used to prevent gas leakage past the sabot body. It has two pins at the front of the sabot to pull the projectile down the barrel. These pins were designed to fit the in-service MPB locator holes.

A pivot pin, which is in line with the saw cuts, was added to force the sabot opening at that point. A polycarbonate ring with a 5° angle is positioned at the aft end of the sabot. There are two reasons for this. The first one, is to have a good pressure seal between the sabot and the gun tube so as to be able to have a known shot start pressure which helps in having consistent muzzle velocities at the same propellant charge mass. The second reason is that, as the sabot leaves the gun tube, the high radial pressure acting on the rear ring relative to the front part, causes the pivoting action at the pivot point of the sabot petals.

A photograph of the sabot-model package as well as all the components is shown in Fig. 3. One should notice the roll pin placed on one of the model fins to make it possible to measure the roll orientation of the projectile when fired in the aeroballistic range. The total model-sabot mass is approximately 5.1 kg. The complete drawings of the sabot as well as the details of the proof trials that were conducted to verify sabot-model integrity at launch can be found in Ref. 8.

3.0 FACILITY DESCRIPTION AND TEST CONDITIONS

3.1 DREV Aeroballistic Range

The DREV aeroballistic range (Refs. 6 and 7) is an insulated steel-clad concrete structure used to study the exterior ballistics of various free-flight configurations. The range complex consists of a gun bay, control room and the instrumented range (Fig. 4a). A massive blast wall is located in front of the building to stop sabot pieces and minimize vibrations transmitted to the range structure and instrumentation. Projectiles of calibers

ranging from 5.56 to 155 mm, including tracer types, may be launched. Large-caliber models have been fired up to Mach 7.

The 230-meter instrumented length of the range has a 6.1-m square cross section with a possibility of 54 instrumented sites along the range (Fig. 4b). For these tests, 41 of the stations were utilized. These sites house fully instrumented orthogonal shadowgraph stations that yield photographs of the shadow of the projectile as it flies down the range. The maximum shadowgraph window, an imaginary circle within which a projectile will cast a shadow on both reflective screens, is 1.6 meters in diameter. There are also four Schlieren stations (two operational for these tests) at the beginning of the range that yield high quality flow photographs. The range is also air conditioned to maintain a constant relative humidity of approximately 45%. The nominal operational conditions of the range are 20° C at standard atmospheric conditions. The spark source and reference point locations that were used were deduced from a standard survey. A dynamic calibration was conducted in the X, Y, X, θ and ψ coordinates.

3.2 Test Conditions and Particularities

Eleven (11) projectiles were fired in the aeroballistic range program with the 110 mm smooth bore gun with the HI-LO adapter (Ref. 8). All the projectiles had roll pins. The range conditions for each test projectile at time of firing are indicated in Table III. The muzzle velocities range from a low of 270 m/s (Mach 0.8) to a maximum of 323 m/s (Mach 0.95). The mid-range Mach numbers varied from 0.68 to 0.83 which yielded Reynolds number, based on the length of projectile, between 6.6×10^6 and 8.0×10^6, respectively. The initial angles of attack ranged from a low of 1.5° to a maximum of 4.5°.

The gun muzzle was situated at a downrange coordinate of approximately 6.32 m in the aeroballistic range coordinate system. Due to the low muzzle velocities, the movable butt was utilized to capture the projectiles before the end of the range. It was

8

placed after the 47th shadowgraph stations at approximately 150.0 m. This allowed a possibility of 41 shadowgraph stations, or 115.0 m, to measure data. This butt was used for all the projectiles.

Due to the length of the models, the total shadow of the projectiles in flight could not be captured on the films. A time delay was deliberately set so that at least the base of the model could be seen with certainty. This allowed the reading of the films at the back of the collar and at the front of the fins for calculating the trajectory.

A typical Schlieren photograph showing the complex flow field and shock structure of a projectile in flight can be seen in Fig. 5 for shot A12 at Mach 0.94.

The numbering scheme to refer to the shots and a particular configuration is as follows. One letter followed by 6 digits, as for example A981002, identifies the shot numbers. The letter corresponds to a particular configuration. The first four numbers (9810) indicate the date (year and month) that the projectile was fired in the range. The last two digits correspond to the shot number for that particular configuration. For the example given above, the shot number corresponds to the second shot of the Model A configuration that was fired in the range in October 1998. For convenience, the shot numbers are usually referred to the letter and the shot number, A02.

4.0 FREE-FLIGHT DATA REDUCTION

Extraction of the aerodynamic coefficients and stability derivatives is the primary goal in analyzing the trajectories measured in the DREV aeroballistic range. This was performed by means of the Aeroballistic Range Facility Data Analysis System (ARFDAS, Ref. 1) described in Fig. 6. These programs incorporate a standard linear theory and a six-degree-of-freedom (6DOF) numerical integration technique. The 6DOF routine incorporates the Maximum Likelihood Method (MLM) to match the theoretical trajectory

with the experimentally measured trajectory. The MLM is an iterative procedure that adjusts the aerodynamic coefficients to maximize a likelihood function. The application of this likelihood function eliminates the inherent assumption in least square theory that the magnitude of the measurement noise must be consistent between parameters (irrespective of units). In general, the aerodynamic coefficients are nonlinear functions of angle of attack, Mach number and roll angle.

ARFDAS represents a complete ballistic range data reduction system capable of analyzing both symmetric and asymmetric models. The essential steps of the data reduction system are to (1) assemble the dynamic data (time, position, angles), model measured physical properties and atmospheric conditions, (2) perform linear theory analysis, and (3) perform 6DOF analysis.

These three steps have been integrated into data analysis system to provide the test scientist with a convenient and efficient means of interaction. At each step in the analysis, permanent records for each shot are maintained so that subsequent analyses with data modification are much faster.

The 6DOF data reduction system can also simultaneously fit multiple data sets (up to five) to a common set of aerodynamics. Using this multiple-fit approach, a more complete range of angle of attack and roll orientation combinations is available for analysis than would be available from a single flight. This increases the accuracy of the determined aerodynamic coefficients over the entire range of angles of attack and roll orientations.

The aerodynamic data presented in this report were obtained using the fixed-plane 6DOF analysis (MLMFXPL) with both the single- and multiple-fit data correlation techniques. The equations of motion have been derived in a fixed-plane coordinate system with Coriolis effects included. The formal derivation of the fixed-plane model is given in Ref. 9.

10

All the results given here were reduced after the dynamic calibration biases were accounted for the X, Y, X, θ and ψ coordinates. The methodology of the dynamic calibration for the DREV aeroballistic range is explained in Ref. 10.

5.0 FREE-FLIGHT RESULTS AND DISCUSSIONS

The aerodynamic coefficients and stability derivatives that were reduced from the free-flight trajectories measured in the aeroballistic range are presented in tabular form for the linear theory analysis and in both tabular and plotted format for the 6DOF reductions. All of the determined aerodynamic coefficients are given at the mid range measured Mach number.

5.1 Linear Theory Results

The linear theory parameters deduced from the decoupled motion are provided in Table IV. The magnitudes of the initial angles of attack varied from a low of 1.6° to a high of roughly 4.5°. The amplitude of the initial nutation and precession arms, KF and KS, and the mean squared yaw (Dbsq) provides an indication of these angles of attack.

In all cases the shots were dynamically unstable, as observed by the positive nutation and precession damping modes (LF and LS). This implies that the angular motion is increasing as the projectile flies downrange. The frequencies (WF and WS) are consistent. It should be noted that the trim angles (KT) are of the order of 0.5° in some cases. This will be further investigated in the 6DOF analysis.

The aerodynamic coefficients deduced from the linear theory parameters are presented in Table V. The methodology to obtain the aerodynamic coefficients is

explained in Ref. 1. The main aerodynamic coefficients (C_{X0}, $C_{N\alpha}$, $C_{M\alpha}$, C_{lp} and $C_{l\delta}$) are consistent. The pitch damping term, C_{Mq}, is positive indicating a dynamic instability for all the shots.

The standard deviation error in the angular motion (E-Ang) from the linear theory analysis (Table V) is high in some cases. The dynamic instability is not well resolved with the linear theory analysis and this suggests that the linear theory analysis was not fitting some parameters adequately, probably due to nonlinear variation with angle of attack in some aerodynamic coefficients. These nonlinearities, if they exist, are best modeled and reduced with the 6DOF reduction technique of the next section.

5.2 Six-Degree-of-Freedom Results

The determined aerodynamic coefficients, their standard deviation errors, and the standard deviation errors between the theoretical and experimental trajectories for the axial, angular and roll motions are given in Tables VI and VII for the single- and multiple-fit data reduction techniques, respectively. The moment reference center for the pitch and moment coefficients was at 46.0% of the length from the nose of the projectile (3.93 cal). All the results are given at the mid-range Mach number for the single-fit data reductions and at the average mid-range Mach numbers for the multiple-fit data reductions.

A coefficient that appears with a value and a (*) between parentheses directly below, indicates that this coefficient was held constant and one that has a (-) between parentheses indicates that this coefficient was solved for and that the standard deviation error for this coefficient was higher than 100%, that is, it does not influence the fit and is considered undetermined. Those with numbers between parentheses represent the standard deviation error for that particular coefficient.

12

The multiple-fit groups were chosen by Mach numbers and three groups of multiple-fit data reductions were conducted, as given in Table VII. In some instances, the results showed more variation in C_{X0} and $C_{M\alpha}$ than would be expected at the same Mach number. Therefore, for some multiple-shot groups, the multiple-fit data reductions were conducted as follows. The axial force coefficient was kept constant at the average of the single-fit results. The variation from this value was then uniquely solved for each shot. A unique $C_{M\alpha}$ was solved for each individual shot in the cases where the variation was deemed too high. It is believed that these variations originate from the flow over the fins due to the high drag collar located at the front of the model. These would be dependent on the angle of attack and roll orientation of the projectile.

As seen from Tables VI and VII, all of the main aerodynamic coefficients (C_{X0}, $C_{N\alpha}$, $C_{M\alpha}$ and C_{Mq0}) were very well determined, as indicated by the low probable errors of fits on the coefficients. It should be noticed that the C_{Mq0} values are positive. The pitch damping quadratic coefficient expansion term ($C_{M_{q_{\alpha}2}}$) was well determined in the multiple-fit data reductions at Mach 0.8 and 0.82. The single fit $C_{M_{q_{\alpha}2}}$ was held constant at the determined multiple values and C_{Mq0} was solved for.

Since there was no fin cant on the projectiles, the roll motion was very limited. Therefore, the roll damping moment, C_{lp}, was kept constant at the PRODAS (Ref. 11) estimates obtained for the MPB-LD bomb (Ref. 12) and the roll producing moment due to fin cant, $C_{l\delta\delta}$, was allowed to vary to take into account any manufacturing tolerances in the fin angles. The aerodynamic trims for the pitch moment and the normal force were solved for all the shots.

13

The yaw axial force ($C_{X_{\alpha^2}}$) was also well resolved in the multiple-fit data reduction and the respective single fits were held constant at the multiple-fit determined value. A pure side moment (C_{nsm}) was resolved in two multiple shot groups. There is no doubt that this side moment originates from the severe turbulence caused by the collar on the fins. The projectile roll motion was almost nothing in most cases.

The standard deviation errors of the single and multiple fits are of the order of 2.5 mm in the downrange coordinate, 1.0 mm in the swerve motion, 0.6° in pitch and yaw and of the order of 5.0° in roll. These errors of the fits in pitch and yaw and in the swerve direction are a bit high when compared with other test programs conducted in the DREV aeroballistic range. The aerodynamic coefficient expansions utilized is probably not as well suited to analyze these type of flows. The 6DOF probable errors of fits are a bit smaller than the linear theory ones because of the better mathematical modeling of the motion, such as the inclusion of aerodynamic trims, angle of attack dependent terms and variations with Mach number.

5.3 Comparison of 6DOF Single- and Multiple-Fit Results

A comparison of the reduced aerodynamic coefficients from the 6DOF data reductions techniques with the single- and multiple-fit results are given in Figures 7 to 13. The single fit data points (AB - SF) are shown as open triangles while the multiple-fit data reduction results (AB - MF) are given as solid triangles.

Appendix A presents, for every test shot, the total angle of attack history with the observed angular motion and the theoretical determined one with the reduced aerodynamic coefficients. The experimental data points (open circles) and the calculated trajectory (continuous line) from the determined coefficients are compared. This allows a verification that the reduced aerodynamic coefficients do fit the experimental trajectory

14

satisfactorily. For every shot, the total angle of attack and the angular motion plots in pitch and yaw are given as a function of the downrange coordinate.

The axial force coefficient at zero angle of attack (C_{X0}) as a function of Mach number is shown in Fig. 7a. C_{X0} is of the order of 3.5 with a high scatter in the single-fit results. The 2nd order axial force coefficient term, $C_{X_{\alpha^2}}$, was well determined and C_X as a function of angle of attack for the three groups of multiple fits is shown in Fig. 7b.

An analysis was conducted for every shot to investigate trends with angles of attack. The data was fit by sections (groups of 15 stations) for different lengths along the range as provided below:

1st station	Last station
1	15
7	21
13	27
19	33
25	39

The total axial force coefficient as a function of the mean angle of attack is shown in Fig. 7c. The variation of C_X as a function of the mean angle of attack is linear. The total C_X determined for the multiple fits as well as an attempt to a fourth order expansion ($C_{X_{\alpha^4}}$ = -10000.0) is superimposed on the sectional data. The fourth order expansions term appears to better fit the data, but the aeroballistic range observed angles of attack were not high enough to confirm this hypothesis.

$C_{N\alpha}$, the normal coefficient slope versus Mach number is displayed in Fig. 8. There is a slight scatter in the single-fit results and $C_{N\alpha}$ is about 15.0 over the whole Mach number range tested.

The variation of the pitching moment coefficient slope, $C_{M\alpha}$, with Mach number is shown in Fig. 9. There is only a very slight scatter in the single-fit results for $C_{M\alpha}$ and it is roughly -50.0 between Mach 0.65 and 0.82.

The total pitch damping coefficient is defined as

$$C_{Mq} = C_{Mq0} + C_{M_{q_{\alpha^2}}} \varepsilon^2$$

The variation of the pitch damping moment coefficient at zero angle of attack, C_{Mq0}, and the second order expansion term, $C_{M_{q_{\alpha^2}}}$, with Mach number are shown in Fig. 10a and Fig. 10b, respectively. As explained previously, C_{Mq0} is positive since the angular motion increases with range and the very high negative values of $C_{M_{q_{\alpha^2}}}$ controls the amplitude of the limit cycle. The variation in the numbers are quite high since no final limit cycles were achieved in the short range of the tests and the angular motion keeps increasing.

C_{Mq} as a function of angle of attack for the three multiple data reductions are shown in Fig. 10c. As the angle of attack increases C_{Mq} crosses the zero barrier at roughly 3.0°. The angular motion can best be explained with the linear theory analysis formulation (Ref. 11). The pitch and yaw motions are modeled by a damped sinusoidal function. The yaw damping factors of the nutation and precession arms for a non-rolling projectile with no side moments and induced moment terms are given by:

$$\lambda_N, \lambda_P = \frac{\rho A}{4 m} \left[-C_{N\alpha} + 2 C_D + \frac{k_t^{-2}}{2} C_{Mq} \right]$$

where

$$k_t^{-2} = \frac{md^2}{I_y}$$

For low drag projectiles the $(2 C_D)$ term is often neglected since it is small compared with $C_{N\alpha}$. This is not the case for this high drag configuration.

The criterion for a projectile to be dynamically stable is that the fast and slow arms damping factors be negative. Dynamic stability boundaries for the fast and slow arms (which are the same in this case) for the pitch damping coefficient can be calculated from the above as:

$$C_{Mq} (\lambda_N = 0.0, \lambda_P = 0.0) = 2 \left[C_{N\alpha} - 2 C_D \right] k_t^2$$

Using $C_D = 3.5$ and $C_{N\alpha} = 15.0$, yields a stability bound for C_{Mq} of roughly 39.0. If this stability bound is superimposed on Fig. 10c, it can be seen that the crossover point is of the order of 3.0° to 4.0°. This agrees quite well with the motion plots at the mid-range value.

The total pitch damping as a function of the mean angle of attack is shown in Fig. 10d. There is no apparent pattern of C_{Mq} as a function of the mean angle of attack for the different sections.

17

C_{l_p} , the roll damping coefficient, is demonstrated versus Mach number in Fig. 11. This term was not solved for due to the lack of roll motion. These are the same values as the MPB-LD (Ref. 12), which were obtained from the predicted values from PRODAS (Ref. 13) and it is about -3.9.

The trim moment and trim normal force coefficients were well determined (Table VI) and they improved the fit noticeably when they were included in the fitting process. The asymmetries caused by modular design of the MPB-HD and the manufacturing tolerances contribute mostly to these coefficients. A trim angle can be calculated separately from the force and the moment term. The total moment trim is:

$$C_{M\delta}\delta_T = \sqrt{(C_{M\delta}\delta_A)^2 + (C_{M\delta}\delta_B)^2}$$

with the total trim angle calculated as:

$$\delta_T = \arcsin\left(\frac{C_{M\delta}\delta_T}{C_{M\alpha}}\right)$$

The force trims are calculated in the same manner. The trend of the total trim angle from the force and moment calculations is shown in Fig. 12 versus Mach number and the magnitudes are not the same from the two different methods at the same Mach number. Usually, the trim moments are better resolved than the normal force trims. In most cases, the trim angles varied from roughly 0.3° to a high of 0.5°. The scatter in the results is also expected since two bombs will not be exactly the same.

UNCLASSIFIED
18

6.0 COMPARISON WITH OTHER EXPERIMENTAL RESULTS

The MPB-HD was extensively tested in the DREV indraft wind tunnel (Ref. 14) during the design phase of the project and as well from full-scale aircraft free-flight trials (Ref. 15). The MPB-HD was also one of the configurations that were utilized in the Open Jet Facility (Ref. 2) that successfully showed that it was possible to extract store separation interference coefficients and free stream aerodynamic coefficients (static and dynamic), simultaneously with the MLM methodology.

The reference center of gravity for the moment coefficient was taken to be the aeroballistic range one, that is 3.94 cal from the nose. The tabulated data from the wind tunnel, Open Jet Facility and from the full-scale free-flight trials can be found in Table VIII. The aerodynamic coefficients measured from the four experimental techniques; the aeroballistic range (AB-SF, AB-MF), the DREV indraft wind tunnel (WT), the Open Jet Facility (OJF) and the full-scale tests (FF - M2470); are compared in Fig. 13. The full-scale tests only provided the total drag coefficient.

The axial force coefficient at zero angle of attack, C_{X0}, is compared in Fig. 13a versus Mach number. The wind tunnel data and the Open Jet Facility results agree extremely well with the aeroballistic range data from Mach 0.7 to 0.9. The full-scale results is slightly above the aeroballistic range results by 15%. It should be noted that full-scale results are for total C_D and since the projectile flies at a certain limit cycle, it would be expected that the results would be higher than the C_{X0} results.

$C_{N\alpha}$, the normal coefficient slope versus Mach number is displayed in Fig. 13b for three of the experimental techniques. The wind tunnel and Open Jet Facility data is within the scatter of the aeroballistic range results.

19

The variation of the pitching moment coefficient slope, $C_{M\alpha}$, with Mach number is shown in Fig. 13c. The lone Open Jet Facility data point as well as the wind tunnel results agrees very well with the Mach number range of the aeroballistic range data

6.1 Limit Cycle Amplitude

As seen from these aeroballistic range results, the MPB-HD is dynamically unstable at low angles of attack. The motion plots (Appendix A) show that, in most cases, the amplitude at 150.0 m downrange is of the order of 6.0° to 8.0° and still increasing but leveling out in some cases. In these aeroballistic range trials, the initial angles of attack were -relatively low.

The angular motions that were obtained in the Open Jet Facility tests (Ref. 2) at roughly Mach = 0.75 had high initial angles of attack that damped (Fig. 14). The angular motion presented is only in one plane and if the projectile were slightly rolling, that would show as low angles of attack in one plane of view, as in Fig. 14a. Nevertheless, the motion is definitely damping but, due to the short time frame of the tests, the final amplitude of the angular motion was not observed.

From both of these tests, the final limit cycle amplitude can be approximated to be between 8.0° to 12.0°. The impact of this limit cycle amplitude on the range and dispersion of the MPB-HD is difficult to assess. Most of the motion plots show a planar motion at random orientations from test to test, and there is no doubt that this will have an impact on the dispersion of this bomb.

7.0 CONCLUSIONS AND RECOMMENDATIONS

The aerodynamic characteristic of a the Modular Practice Bomb - High Drag (MPB-HD) or the BDU-5002/B MOD 1 were determined from free-flight tests conducted in the DREV aeroballistic range. Eleven projectiles were successfully fired in the Mach number range of 0.6 to 0.8. The aerodynamic coefficients and stability derivatives (C_{X0}, $C_{N\alpha}$, $C_{M\alpha}$, and $C_{l\delta}\delta$) were well determined. The measured angular motion showed that this projectile is dynamically unstable at low angles of attack. The pitch damping coefficient at zero angle of attack (C_{Mq0}) and the second order expansion term ($C_{Mq_{\alpha^2}}$) were well determined. The yaw axial force term as well as pure side moments and the trims were also reduced. A dynamic stability analysis was also conducted.

Wind tunnel, Open Jet Facility experimental results as well as full-scale tests were compared with the aeroballistic range results. The static aerodynamic coefficients from these three experimental techniques agreed very well with the aeroballistic range data.

From these aeroballistic range tests and the Open Jet Facility experiments, the final limit cycle amplitude of the MPB-HD can be approximated to be between 8.0° to 12.0°. The impact of this limit cycle amplitude on the range and dispersion of the MPB-HD is difficult to assess. Most of the motion plots show a planar motion at random orientations from test to test, and there is no doubt that this will have an impact on the dispersion of this bomb.

Due to the complex shape of the MPB-HD, it was not possible to obtain aerodynamic predictions from semi-empirical/analytical codes since it lies outside their scope of application. It was not deemed necessary to conduct CFD calculations for this configuration.

This database of aerodynamic coefficients generated by this experimental program is considered a success. When it is combined with the wind tunnel, Open Jet Facility and full-scale free-flight trials, it can be used with the BSSM, the SSM as well as the DREV 6DOF trajectory program to predict accurate weapon performance. Also, it can be exploited with confidence for the CF-18 OFP. The methodology should be extended to other weapon systems.

8.0 ACKNOWLEDGEMENTS

UNCLASSIFIED
22

9.0 REFERENCES

1. "ARFDAS97", Version 4.11, Arrow Tech Associates Inc, August 1997.

2. "Open Jet Facility Data Analysis System (OJFDAS)", Arrow Tech Associates Inc., DREV Contract No. W7701-0-1227, March 1992.

3. "Development of the MLM with Interference Coefficients and Tabular Aerodynamics for SSMDAS", Arrow Tech Associates, DREV contract No. W7701-5-2059, March 1996

4. Stathopoulos, N. and Ouellet, M., "Implementation of MLM for Store Separation Work - Phase II", Bombardier document MAU-261-213, May 1998

5. Jiang, L-J., "Advances in Aircraft/Store Separation Methodologies", NRC, LTR-A-001, October 1995

6. Drouin, G., Dupuis, A. and Côté, F., "Instrumentation Development and Data Analysis for the DREV Aeroballistic Range", DREV M-2800/87, March 1987, UNCLASSIFIED

7. Dupuis, A. and Drouin, G., "The DREV Aeroballistic Range and Data Analysis System", AIAA Paper No. 88-2017, AIAA 15th Aerodynamic Testing Conference, San Diego, California, 18-20 May, 1988.

8. Dupuis, A. D. and Normand, M., "Sabot Performance for Gun Launched MK-82 CF, BDU-5003/B and BDU-5002/B Bombs", DREV-TM-9734, January 1998, UNCLASSIFIED

UNCLASSIFIED
23

9. Hathaway, W. H. and Whyte, R., "Aeroballistic Research Facility Free-Flight Data Analysis using the Maximum Likelihood function", AFATL-TR-79-98, December 1979, UNCLASSIFIED.

10. Whyte, R. and Hathaway, W., "Dynamic Calibration of Spark Aeroballistic Ranges", 44th Aeroballistic Range Association Meeting, 13-17 September., 1993, Munich.

11. Winchenbach, G. l., "Aerodynamic Testing in a Free-Flight Spark Range", WL-TR-1997-7006, April 1997.

12. Dupuis, A. D., "Aerodynamic Characteristics of the BDU-5002/B MOD 1 Bomb at Subsonic and Transonic Velocities from Aeroballistic Range Free-Flight Tests", DREV TR-2000-115, November 2000, UNCLASSIFIED

13. "Projectile Design Analysis System (PRODAS), PC Version 3.9", Arrow Tech Associates Inc., 1995.

14. Girard, B., Drouin, G. and Cheers, B., "Supersonic Wind Tunnel Tests (MPBWT-5) of the Modular Practice Bomb", DREV M-2662/84, June 1984, UNCLASSIFIED

15. Girard, B., Cheers, B. and Lepage, R., "The Modular Practice Bomb as a Training Simulator for the BL-755 Cluster Bomb", DREV M-2740/85, August 1985, UNCLASSIFIED

UNCLASSIFED

TABLE I
Nominal physical properties of model

d (mm)	m (g)	I_x (g-cm^2)	I_y (g-cm^2)	l (mm)	CG from nose (% /100)
50.8	2730.7	10286.1	171702.0	434.34	0.46

TABLE II
Physical properties of test projectiles

Model #	d (mm)	l (mm)	CG from nose (mm)	CG from nose/l (-)	CG from nose (cal)	m (g)	I_x (g cm^2)	I_y (g cm^2)
A01	50.84	432.131	201.809	0.46701	3.97	2750.9	10296.27	176578.37
A02	50.69	432.817	200.792	0.46392	3.96	2709.6	10141.91	170918.21
A03	50.77	433.198	201.317	0.46472	3.96	2721.2	10213.50	171677.06
A04	50.77	433.122	199.855	0.46143	3.94	2691.1	10156.59	166069.14
A05	50.88	433.376	200.172	0.46189	3.93	2719.4	10360.04	167959.99
A06	50.85	433.503	202.071	0.46613	3.97	2747.3	10388.09	173916.72
A07	50.80	433.274	202.164	0.46660	3.98	2741.3	10243.65	174408.93
A08	50.85	432.588	200.142	0.46266	3.94	2711.2	10221.22	168238.05
A09	50.93	432.207	200.432	0.46374	3.94	2746.6	10338.28	172853.03
A10	50.88	432.512	199.815	0.46199	3.93	2715.9	10312.85	168597.78
A11	50.98	432.791	202.072	0.46690	3.96	2778.7	10425.39	178226.67

UNCLASSIFIED

TABLE III
Range conditions

Shot Number	No of Stations	Observed Distance (m)	Pressure (mbar)	Temperature (degrees C)	Relative Humidity %	Air Density (kg/m3)	Speed of Sound (m/sec)	Reynolds Number
A981001	39	115.0	993.80000	21.13	36.0000	1.1765	343.895	$.657 \times 10^7$
A981002	39	115.0	994.30000	21.20	36.0000	1.1768	343.934	$.670 \times 10^7$
A981003	38	110.0	994.50000	21.04	36.0000	1.1776	343.843	$.700 \times 10^7$
A981011	38	115.0	988.00000	21.11	35.0000	1.1697	343.882	$.734 \times 10^7$
A981004	37	115.0	984.16000	21.13	39.0000	1.1650	343.897	$.734 \times 10^7$
A981010	39	115.0	988.00000	21.33	35.0000	1.1688	344.014	$.758 \times 10^7$
A981006	37	115.0	984.40000	21.61	39.0000	1.1634	344.173	$.756 \times 10^7$
A981005	38	115.0	984.10000	21.42	39.0000	1.1638	344.062	$.764 \times 10^7$
A981008	18	62.6	981.00000	21.33	41.0800	1.1605	344.014	$.787 \times 10^7$
A981007	34	115.1	982.00000	21.25	41.0000	1.1620	343.967	$.790 \times 10^7$
A981009	37	115.0	987.40000	21.20	36.0000	1.1686	343.937	$.795 \times 10^7$

TABLE IV
Linear theory analysis parameters

Shot No	Mach No.	Dbsq deg^2	KF deg	KS deg	LF 1/m	LS 1/m	WF deg/m	WS deg/m	WDF deg/m^2	WDS deg/m^2	KT deg	E-ANG deg
A981001	.682	9.23	1.37	1.89	.0062	.0036	24.40	-24.51	-.011	.021	.168	.272
A981002	.694	3.93	.68	1.39	-.0107	.0059	30.11	-26.38	-.151	.025	.046	.400
A981003	.723	11.98	2.51	2.09	-.0016	.0039	23.84	-23.91	.000	.000	.084	.365
A981011	.766	13.26	1.73	2.21	.0082	.0011	24.85	-24.36	-.018	.012	.132	.553
A981004	.766	6.08	1.95	2.02	.0001	-.0053	24.63	-24.30	-.004	.004	.151	.389
A981010	.792	18.91	2.98	2.03	.0014	-.0063	24.78	-24.59	-.009	.009	.209	.468
A981006	.792	5.67	1.92	1.53	-.0049	.0037	22.48	-22.89	.019	-.009	.257	.380
A981005	.784	9.10	1.75	1.01	-.0054	.0105	24.06	-23.49	.000	-.002	.230	.317
A981008	.830	4.21	1.70	.77	.0030	.0030	22.68	-18.80	.040	-.070	.243	.429
A981007	.828	15.38	1.90	2.80	.0024	.0026	23.49	-23.27	-.001	-.007	.474	.506
A981009	.831	12.40	1.63	1.87	.0050	.0068	22.83	-22.90	.017	-.013	.111	.425

UNCLASSIFIED

TABLE V
Linear theory aerodynamic coefficients

Shot No.	Mach No.	Dbsq deg^2	CX0	CX2	CNa	Cma	Cmq	Cnpa	Cld	Clp	Clpw	E-X m	E-SWR m	E-ANG deg	E-PHI deg
A981001	.682	9.2	3.841	1.84	14.79	-49.35	185.7	.01	.0080	-4.1120	.0000	.0012	.0016	.272	4.36
A981002	.694	3.9	3.764	1.88	23.17	-46.12	59.8	.01	.0005	-4.1276	.0000	.0035	.0061	.400	4.31
A981003	.723	12.0	3.955	1.95	16.75	-49.33	107.3	.01	.0022	-4.1642	.0000	.0033	.0034	.365	6.55
A981011	.766	13.3	3.973	2.05	19.19	-51.01	204.4	.01	.0006	-4.2175	.0000	.0039	.0024	.553	6.87
A981004	.766	6.1	3.780	2.05	14.63	-49.74	13.3	.01	.0047	-7.8590	.0000	.0028	.0038	.389	2.55
A981010	.792	18.9	4.048	2.12	16.22	-50.06	162.5	.01	.0045	-4.1000	.0000	.0029	.0065	.468	3.43
A981006	.792	5.7	3.776	2.12	21.26	-48.93	90.9	.01	.0016	-4.2497	.0000	.0012	.0047	.380	2.46
A981005	.784	9.1	3.789	2.10	23.46	-48.67	288.8	.01	-.0006	-4.2405	.0000	.0023	.0052	.317	4.78
A981008	.830	4.2	3.646	2.36	12.04	-43.29	124.7	.01	-.0016	-4.3190	.0000	.0007	.0013	.429	2.90
A981007	.828	15.4	3.985	2.35	16.78	-49.37	141.1	.01	.0056	-4.3163	.0000	.0032	.0037	.506	2.35
A981009	.831	12.4	3.878	2.37	15.48	-49.42	209.8	.01	.0005	-4.3224	.0000	.0026	.0014	.425	2.74

TABLE VI
Six-degree-of-freedom aerodynamic coefficients – Single fits

Shot Number	Mach Number	DBSQ / ABARM	CX / CX2	CNa / CNa3	CYpa / Cnpa	Cma / Cma3	Cmq / Cmq2	CZga3 / Cmga3	CYga3 / Cnga3	Clga2 / Cnsm	Clp / Cld	CNda / CNdB	Cmda / CmdB	X(m) / Y-Z(m)	Angle(deg) / Roll(deg)
A981001	.684	9.7	3.543 (0.8%)	15.60 (7.%)	.00 (*)	-50.696 (0.%)	270.1 (8.%)	.0 (*)	.0 (*)	.00 (*)	-4.112 (*)	.000 (*)	.048 (27.%)	.0010	.414
		4 8	100.0 (*)	.0	.0 (*)	.0 (*)	-100000 (*)	.0 (*)	.0 (*)	-.80 (*)	.008 (6.%)	.000 (*)	.001 (-)	.0008	4.072
A981002	.696	4.4	3.696 (0.8%)	17.18 (10.%)	.00 (*)	-54.712 (1.%)	230.0 (*)	.0 (*)	.0 (*)	.00 (*)	-4.128 (*)	-.017 (-)	-.082 (86.%)	.0012	.474
		3.0	100.0 (*)	.0	.0 (*)	.0 (*)	-100000 (*)	.0 (*)	.0 (*)	-1.01 (39.%)	.001 (71.%)	.003 (-)	-.003 (-)	.0005	4.493
A981003	.726	12.6	3.636 (0.8%)	16.45 (6.%)	.00 (*)	-50.858 (0.%)	261.7 (6.%)	.0 (*)	.0 (*)	.00 (*)	-4.164 (*)	.000 (*)	.068 (13.%)	.0011	.316
		4.7	100.0 (*)	.0	.0 (*)	.0 (*)	-100000 (*)	.0 (*)	.0 (*)	-1.04 (13.%)	.002 (32.%)	.000 (*)	-.060 (13.%)	.0008	6.833
A981011	.767	15.1	3.207 (1.8%)	17.22 (5.%)	.00 (*)	-50.571 (1.%)	510.9 (3.%)	.0 (*)	.0 (*)	.00 (*)	-4.217 (*)	-.030 (41.%)	.136 (38.%)	.0011	.336
		5.8	165.0 (*)	.0	.0 (*)	.0 (*)	-135000 (*)	.0 (*)	.0 (*)	-4.36 (23.%)	.000 (-)	-.010 (-)	-.059 (76.%)	.0007	7.191
A981004	.770	6.1	3.588 (0.8%)	16.42 (10.%)	.00 (*)	-50.038 (0.%)	130.4 (22.%)	.0 (*)	.0 (*)	.00 (*)	-4.000 (*)	.002 (-)	-.126 (56.%)	.0014	.476
		3.9	165.0 (*)	.0	.0 (*)	.0 (*)	-135000 (*)	.0 (*)	.0 (*)	.00 (*)	.004 (7.%)	.000 (-)	-.069 (-)	.0006	2.428
A981010	.794	19.2	3.127 (1.8%)	15.33 (9.%)	.00 (*)	-50.094 (0.%)	505.6 (4.%)	.0 (*)	.0 (*)	.00 (*)	-4.100 (*)	.009 (-)	-.062 (-)	.0018	.473
		6 4	165.0 (*)	.0	.0 (*)	.0 (*)	-135000 (*)	.0 (-113.7) (40.%)	-113.7 (40.%)	.00 (*)	.005 (7.8%)(80.%)	-.016 (-)	.123 (51.%)	.0013	3.886

TABLE VI (continued)

Shot Number	Mach Number	DBSQ ABARM	CX CX2	CNa CNa3	CYpa Cnpa	Cma Cma3	Cmq Cmq2	CZga3 Cmga3	CYga3 Cnga3	Clga2 Cnsm	Clp Cld	CNda CNdB	Cmda CmdB	X(m) Y-Z(m)	Standard Error Angle(deg) Roll(deg)
A981006	.794	5.9	3.612 (0.8%)	16.78 (10.8%)	.00 (*)	-49.488 (0.8%)	131.3 (17.8%)	.0 (*)	.0 (*)	.00 (*)	-4.250 (*)	.013 (-)	.132 (38.8%)	.0013	.361
		3.5	100.0 (*)	.0 (*)	.0 (*)	.0 (*)	-100000. (*)	.0 (*)	.0 (*)	-1.34 (14.8%)	.002 (15.8%)	-.042 (40.8%)	-.215 (23.8%)	.0008	2.480
A981005	.802	8.4	3.500 (0.8%)	16.15 (4.8%)	.00 (*)	-50.110 (1.8%)	441.5 (6.8%)	.0 (*)	.0 (*)	.00 (*)	-4.240 (*)	.027 (59.8%)	-.151 (37.8%)	.0007	.388
		5.5	100.0 (*)	.0 (*)	.0 (*)	.0 (*)	-100000. (*)	.0 (*)	.0 (*)	-3.67 (27.8%)	-.001 (80.8%)	-.014 (-)	-.173 (33.8%)	.0003	3.879
A981008	.830	4.3	3.434 (0.8%)	16.17 (*)	.00 (*)	-48.657 (2.8%)	455.0 (*)	.0 (*)	.0 (*)	.00 (*)	-4.319 (*)	.046 (65.8%)	-.143 (80.8%)	.0008	.557
		2.9	165.0 (*)	.0 (*)	.0 (*)	.0 (*)	-135000. (*)	.0 (*)	.0 (*)	-1.58 (49.8%)	-.001 (-)	-.012 (-)	.070 (-)	.0008	3.189
A981007	.831	16.0	3.606 (1.8%)	13.95 (8.8%)	.00 (*)	-51.446 (1.8%)	348.7 (7.8%)	.0 (*)	.0 (*)	-3.34 (9.8%)	-4.316 (*)	-.002 (-)	.270 (28.8%)	.0012	.498
		6.1	100.0 (*)	.0 (*)	.0 (*)	.0 (*)	-100000. (*)	.0 (*)	.0 (*)	-.93 (22.8%)	.008 (4.8%)	.021 (96.8%)	.311 (24.8%)	.0011	1.471
A981009	.833	13.7	3.490 (1.8%)	15.25 (12.8%)	.00 (*)	-49.548 (1.8%)	373.8 (5.8%)	.0 (*)	.0 (*)	.00 (*)	-4.322 (*)	.011 (-)	-.038 (-)	.0022	.427
		6.0	100.0 (*)	.0 (*)	.0 (*)	.0 (*)	-100000. (*)	.0 (*)	.0 (*)	-.85 (22.8%)	.001 (55.8%)	-.016 (80.8%)	.000 (*)	.0013	2.826

UNCLASSIFIED

TABLE VII
Six-degree-of-freedom aerodynamic coefficients – Multiple fits

Shot Numbers	Mach Number	DBSQ ABARM	CX CX2 CX4	CNa CNa3 CNa5	CYpa Cnpa Cnpa3	Cma Cma3 Cma5	Cmq Cmq2 Cmq4	CZga3 Cmga3 Cmga	CYga3 Cnga3 Cnga5	Clga2 CXga2 Clp	CXM CmaM CnsM	Standard Error X(m) Y-Z(m)	Angle(deg) Roll(deg)
A981002 A981001	A981003 .702	8.5 4.7	3.402 (*) 323.1 (17.%) .0 (*)	16.91 (6.%)	.00 (*) .0 (*) .0 (*)	0.0 (*) .0 (*) .0 (*)	227.4 (5.%) -100000. (*) .0 (*)	.0 (*) .0 (*) .0 (*)	.0 (*) .0 (*) .0 (*)	.00 (*) .00 -4.11 (*)	1.48 (53.%) -38.79 (14.%) -.76 (13.%)	.0022 .0007	.428 5.209
A981002			-0.031 (-)										
A981003			-0.597 (40.%)		-54.178 (1.%)								
A981001			-0.363 (48.%)		-49.875 (1.%)								
					-51.391 (1.%)								
A981010 A981011	A981004 .790 A981008	11.1 6.3	3.386 (1.%) 166.1 (6.%) .0 (*)	13.79 (9.%)	.00 (*) .0 (*) .0 (*)	-50.495 (0.%) .0 (*) .0 (*)	447.2 (14.%) -131132. (20.%) .0 (*)	.0 (*) .0 (*) .0 (*)	.0 (*) .0 (*) .0 (*)	.00 (*) .00 (*) -4.32 (*)	.37 (-) .00 (*) .00 (*)	.0037 .0011	.852 4.704
A981005 A981008 A981009	A981006 .818 A981007	9.4 5.8	3.543 (0.%) 105.0 (4.%) .0 (*)	14.42 (5.%)	.00 (*) .0 (*) .0 (*)	-49.792 (0.%) .0 (*) .0 (*)	333.6 (8.%) -111132. (11.%) .0 (*)	.0 (*) .0 (*) .0 (*)	.0 (*) .0 (*) .0 (*)	.00 (*) .00 (*) -4.32 (*)	.47 (33.%) .00 (*) -.91 (16.%)	.0018 .0010	.582 2.937

UNCLASSIFIED

TABLE VIII
Experimental results

a) Full scale free-flight (Ref. 15)

Mach	C_D
0.30	3.66
0.40	3.69
0.50	3.72
0.54	3.75
0.60	3.79
0.66	3.84
0.70	3.88
0.74	3.92
0.80	4.01
0.95	4.80

b) DREV Indraft Wind Tunnel (Ref. 14)

Mach	C_{X0}	$C_{N\alpha}$	$C_{M\alpha}$
0.5	3.437	16.96	-54.50
0.6	3.393	16.27	-52.94
0.7	3.363	15.70	-51.05
0.8	3.339	14.78	-49.16
0.9	4.685	19.02	-62.40
1.5	5.177	14.27	-40.23

c) DREV Open Jet Facility (Ref. 2)

Mach	C_{X0}	$C_{N\alpha}$	$C_{M\alpha}$
0.83	3.379	18.12	-48.09

UNCLASSIFIED

FIGURE 1 - MPB-HD geometry for aeroballistic range tests
(all dimensions in caliber, 1 cal = 50.8 mm)
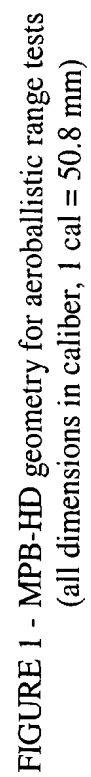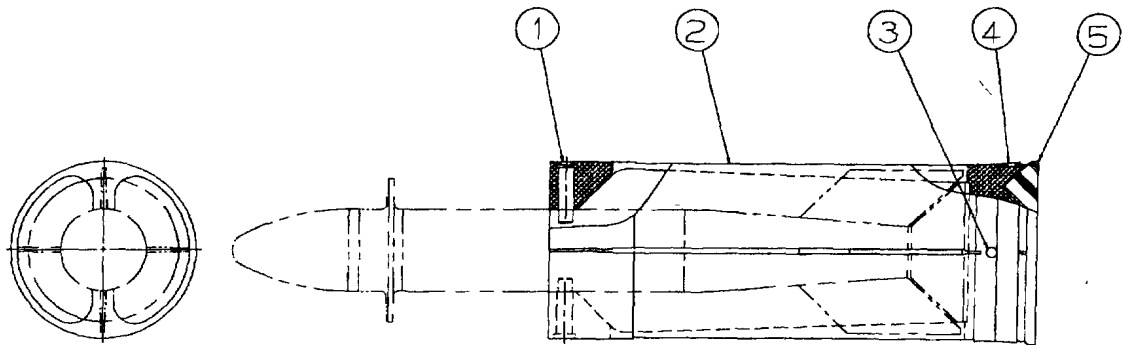
FIGURE 2 - Sabot schematic for the MPB-HD projectile
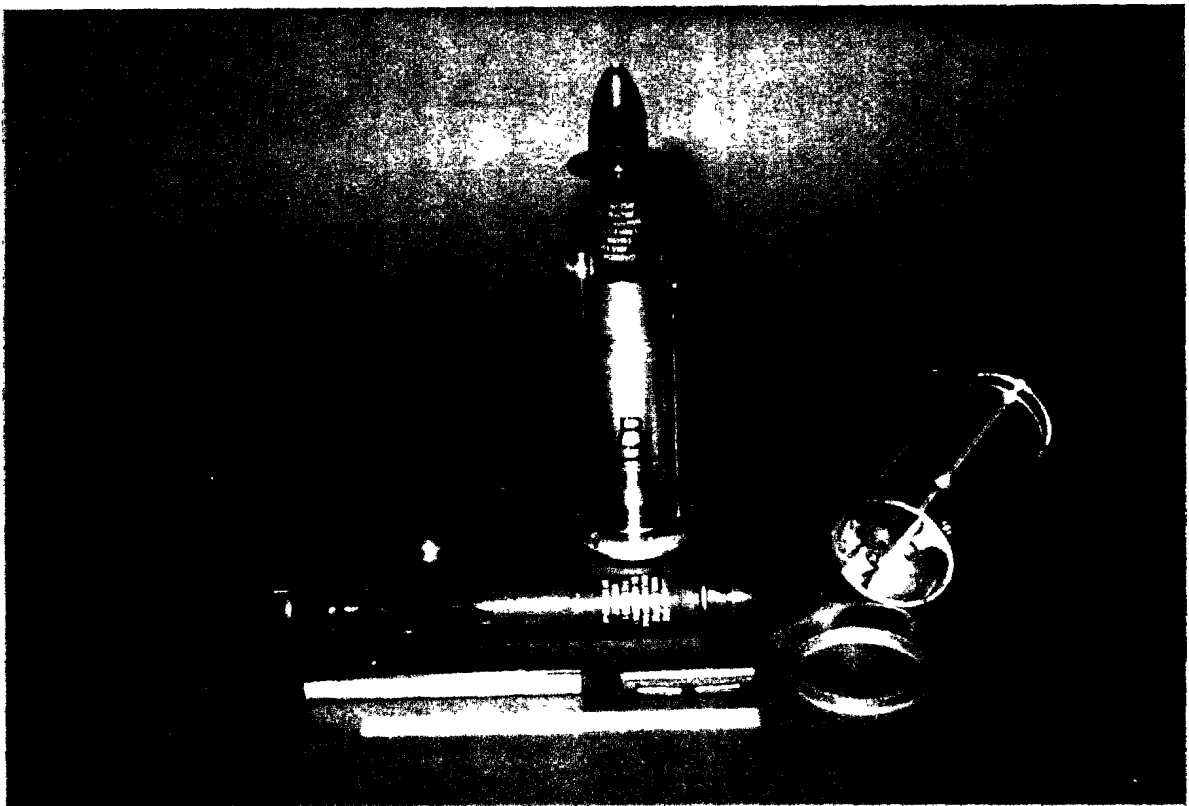
FIGURE 3 - Photograph of model and sabot package for the MPB-HD bomb

FIGURE 4 - DREV aeroballistic range

Fig. 4a) Photograph of aeroballistic range complex
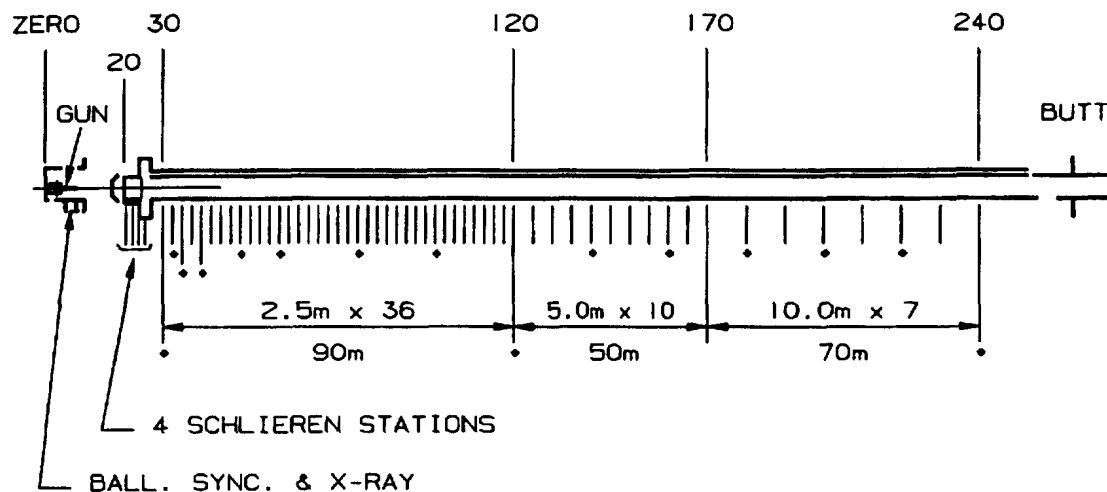
Fig. 4b) Photographic station spacing

UNCLASSIFIED

FIGURE 5 - Typical Schlieren photograph for MPB-HD - Shot A12 (M = 0.9)
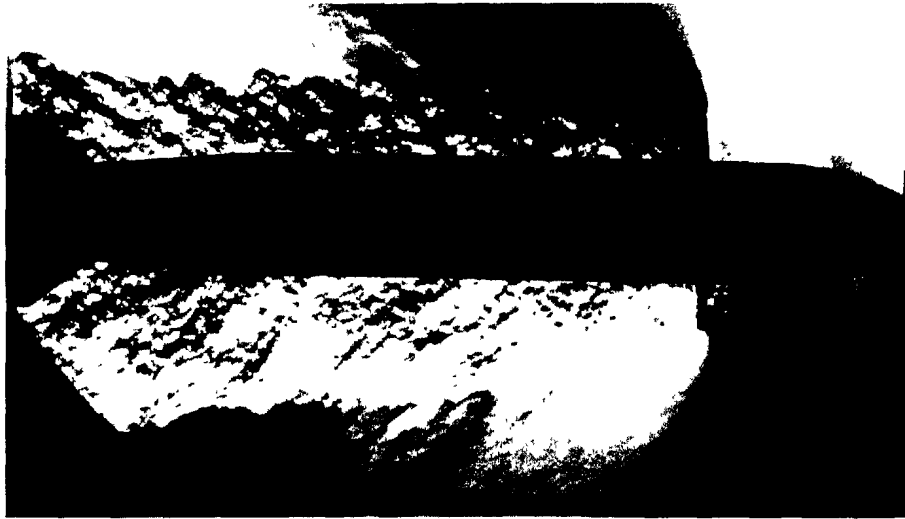
a) Station S24

b) Station S26

ARFDAS - *Aeroballistic Range Facility Data Analysis*

6DOF Dynamic Data

$$t, x, y, z, \phi, \theta, \psi$$

Physical Properties

$$L, M, D, I_x, I_y, I_z$$
$$I_{xy}, I_{xz}, I_{yz}$$

Atmospheric Conditions

$$\rho, P, T, \mu$$

ARFDAS Startup

Linear Theory Analysis

Fit Theoretical to Experimental

Single & Multiple Fits

6DOF Symmetric or 6DOF Asymmetric

Aerodynamic Forces & Moments vs. Mach No. & Angle of Attack & Roll Angle

$$C_{Xo}, C_{X\alpha2}, C_{X\alpha4}, C_{N\alpha}, C_{N\alpha3}, C_{N\alpha5}, C_{Yp\alpha}, C_{Yp\alpha3}\cdots$$
$$C_{m\alpha}, C_{m\alpha3}, C_{m\alpha5}, C_{mq}, C_{mq2}, C_{np\alpha}, C_{np\alpha3}, C_{np\alpha5}\cdots$$
$$C_{n\beta}, C_{n\beta3}, C_{nr}, C_{nr2}, C_{n\alpha}, C_{m y\alpha3}, C_{n y\alpha3}$$
$$C_{\ell p}, C_{\ell p\alpha2}, C_{\ell\delta}\delta, C_{\ell y\alpha3}\cdots\cdots$$
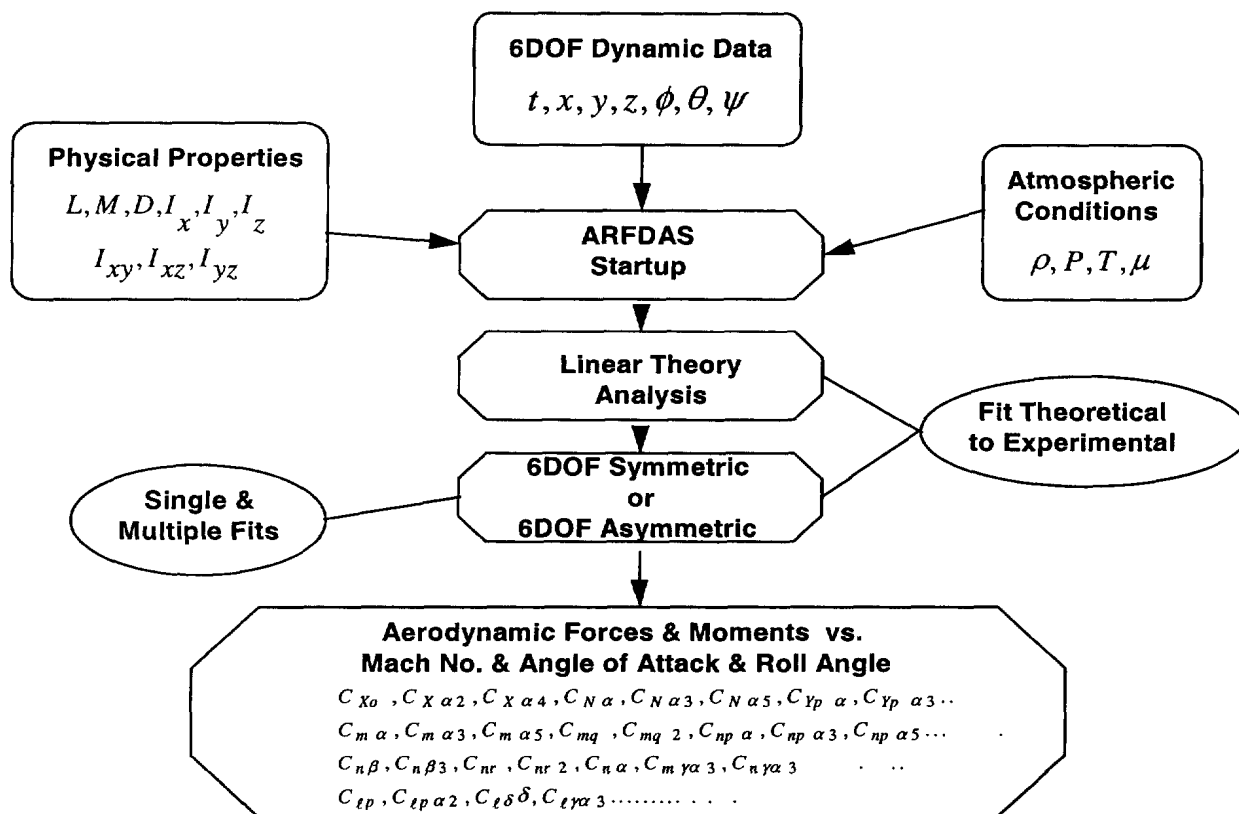
FIGURE 6 - DREV Aeroballistic Range Facility Data Analysis System

FIGURE 7 – Axial force coefficient
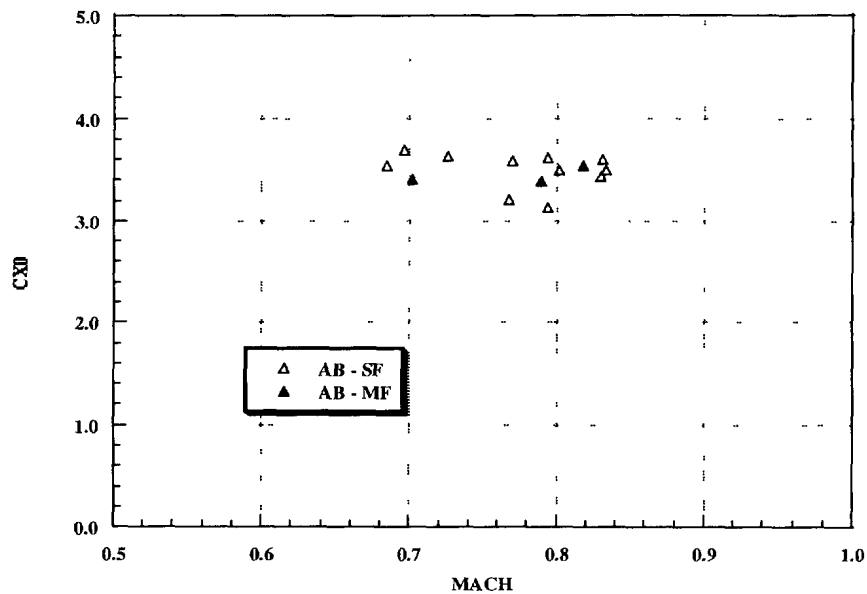
Fig. 7a) C_{X0} versus Mach number
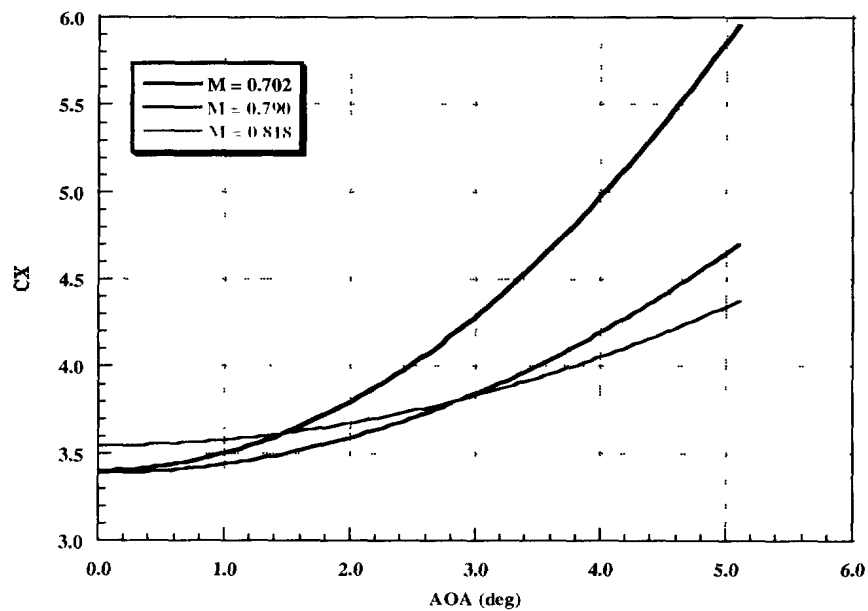
Fig. 7b) C_X versus angle of attack

UNCLASSIFIED
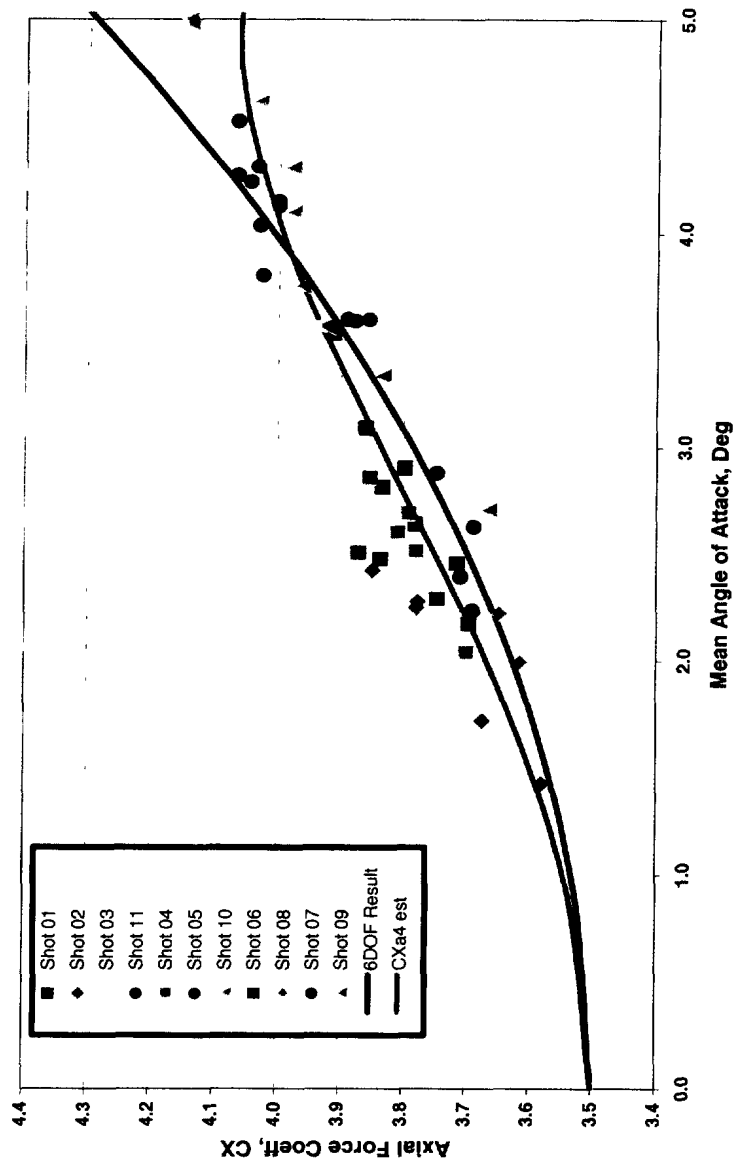
Fig. 7c) C_X versus mean angle of attack

UNCLASSIFIED
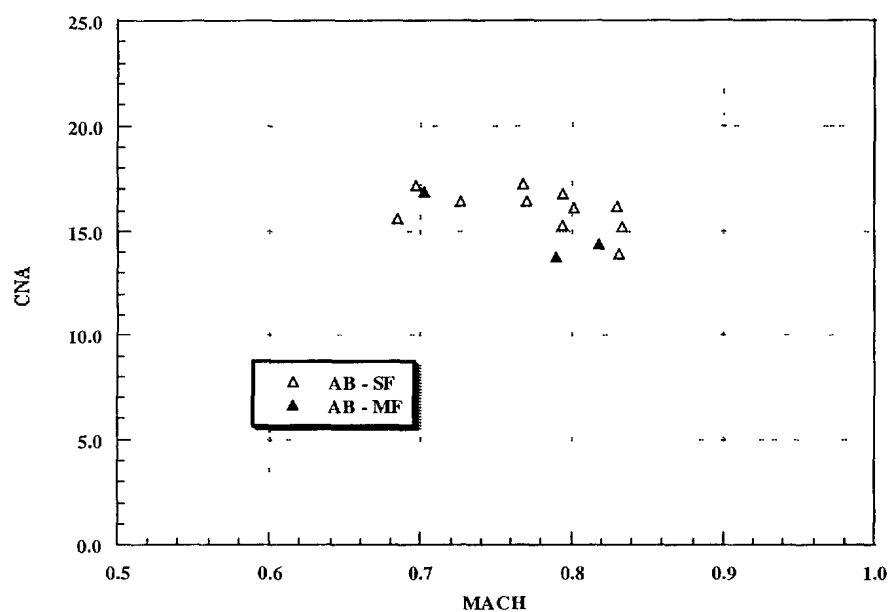
FIGURE 8 - Normal force coefficient slope versus Mach number
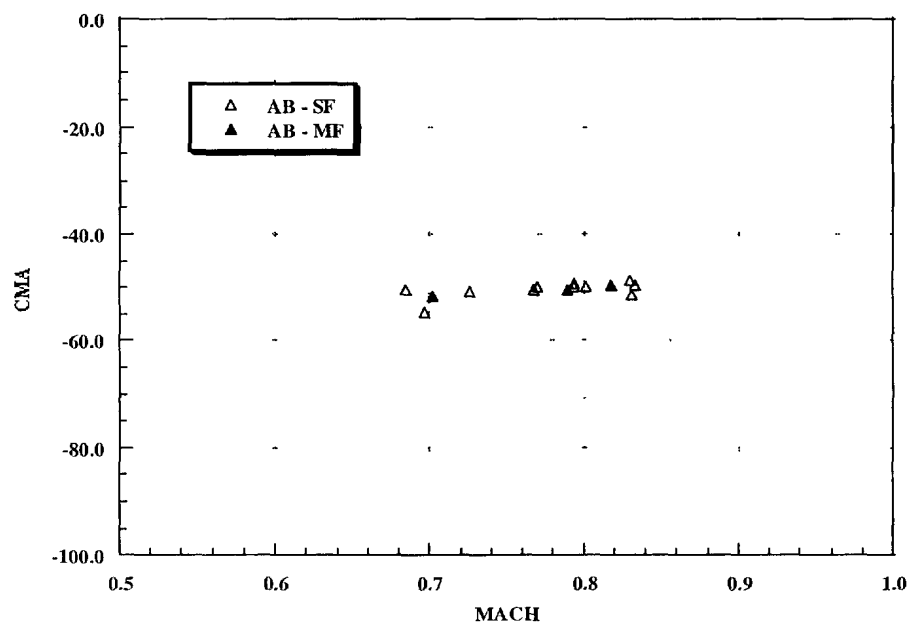
FIGURE 9 - Pitch moment coefficient slope versus Mach number

FIGURE 10 – Pitch damping coefficient
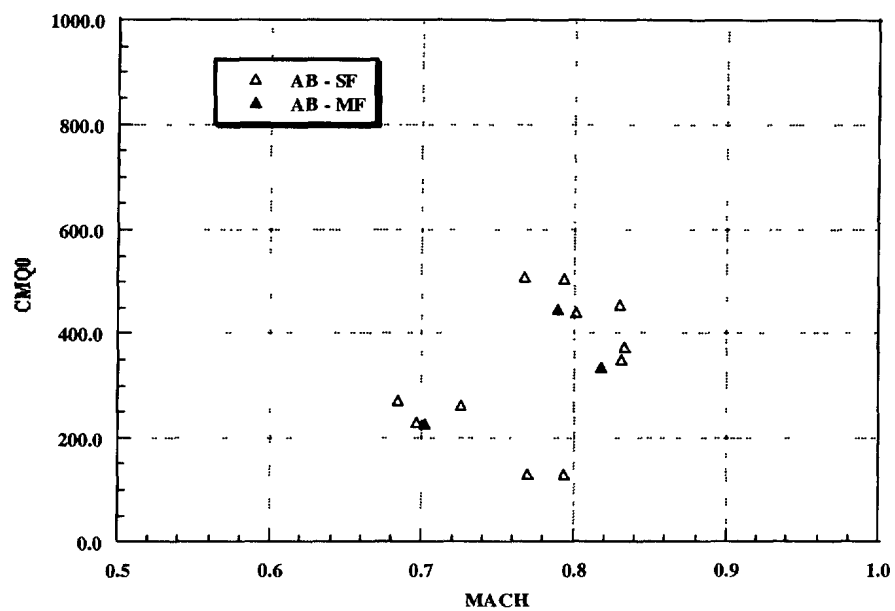
Fig. 10a) C_{Mq0} versus Mach number
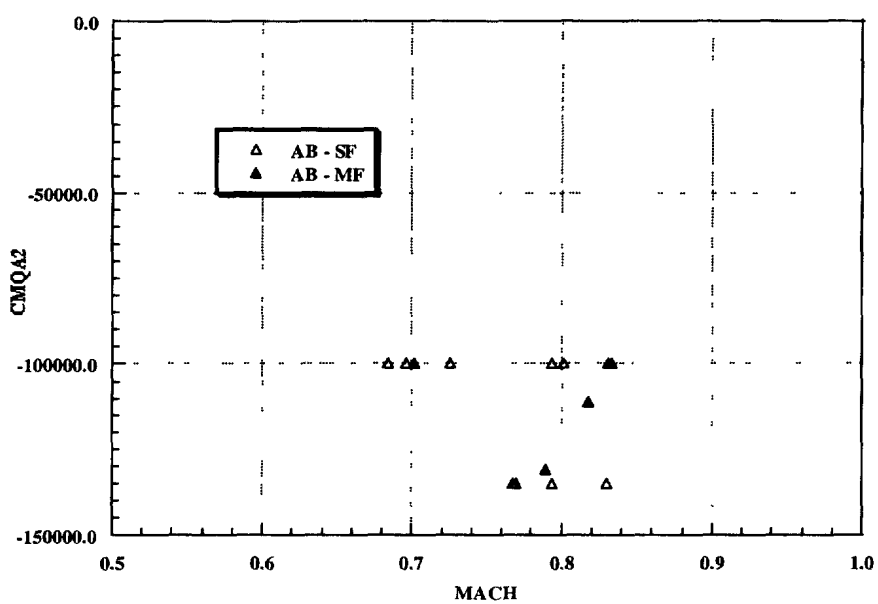
Fig. 10b) $C_{Mq_\alpha 2}$ versus Mach number

UNCLASSIFIED
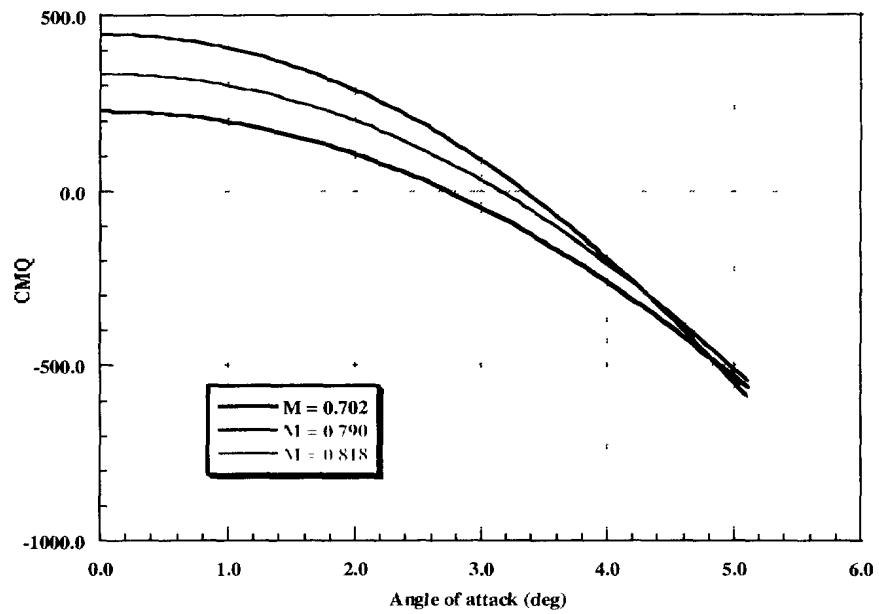
Fig. 10c) C_{Mq} versus angle of attack
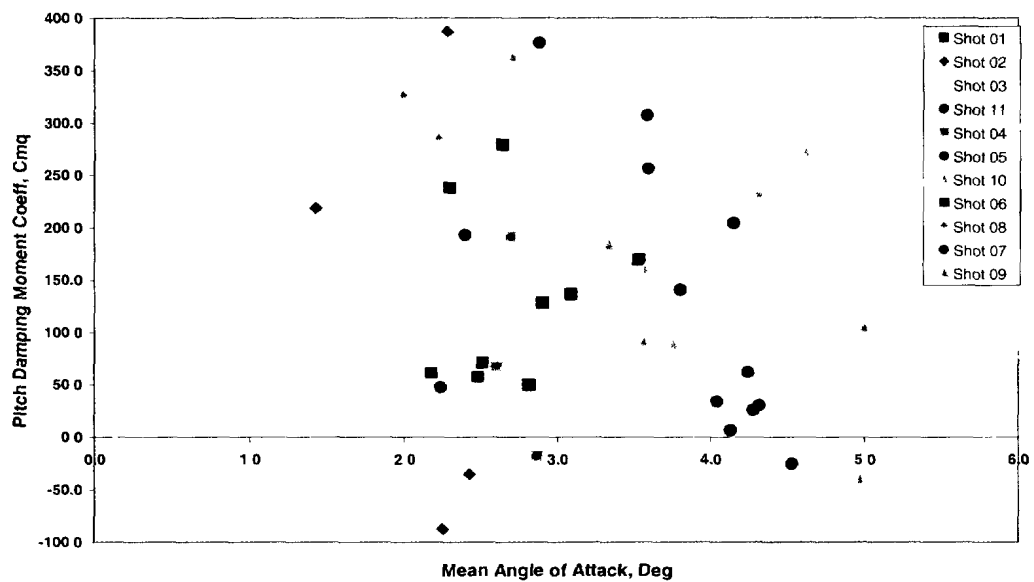
Fig. 10d) C_{Mq} versus mean angle of attack
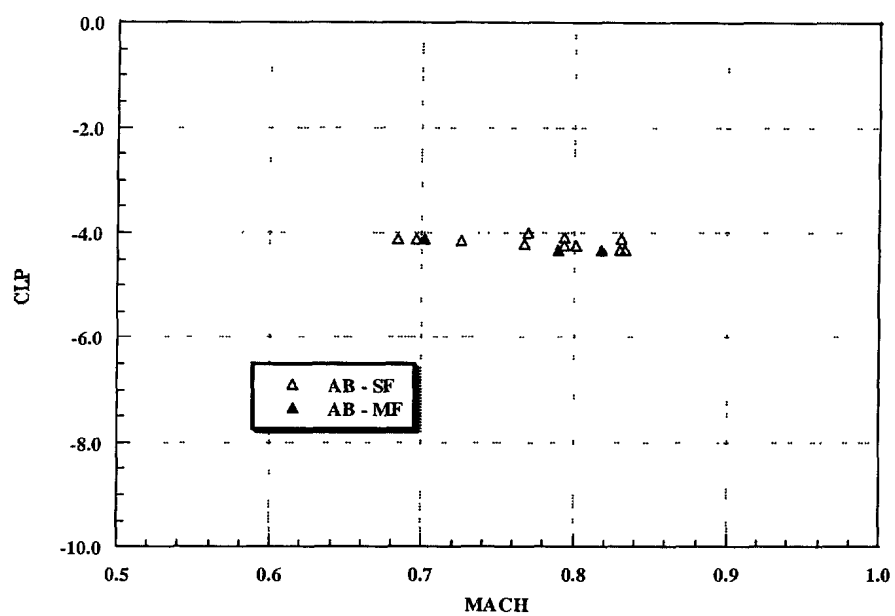
FIGURE 11 - Roll damping coefficient
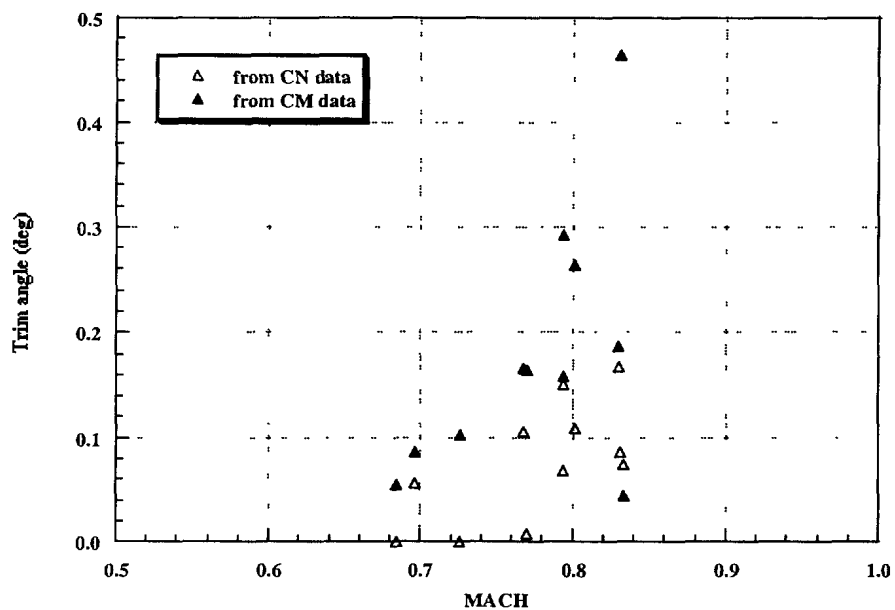
FIGURE 12 - Trim angle

FIGURE 13 – Comparison of experimental results versus Mach number
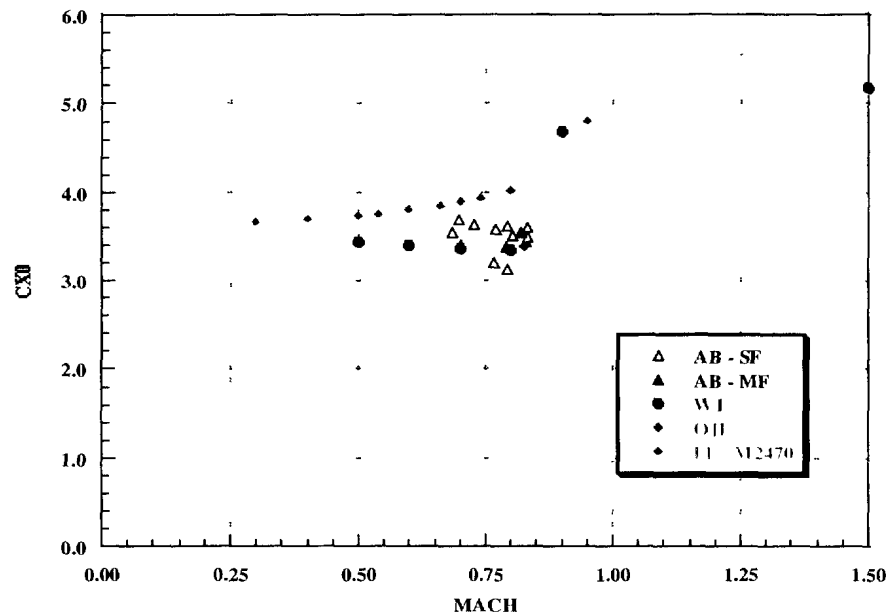
Fig. 13a) Axial force coefficient
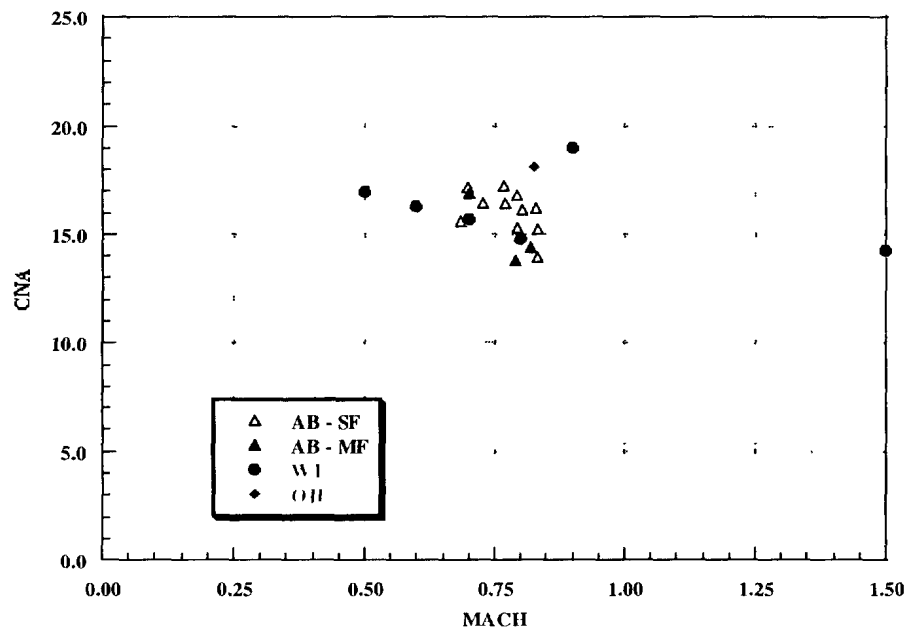
Fig. 13b) Normal force coefficient slope

Fig. 13c) Pitch moment coefficient slope

UNCLASSIFIED

APPENDIX A

Angular Motion Plots
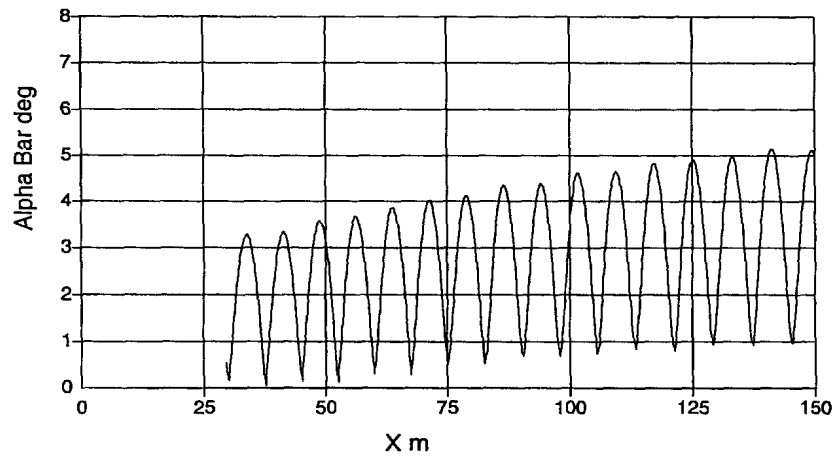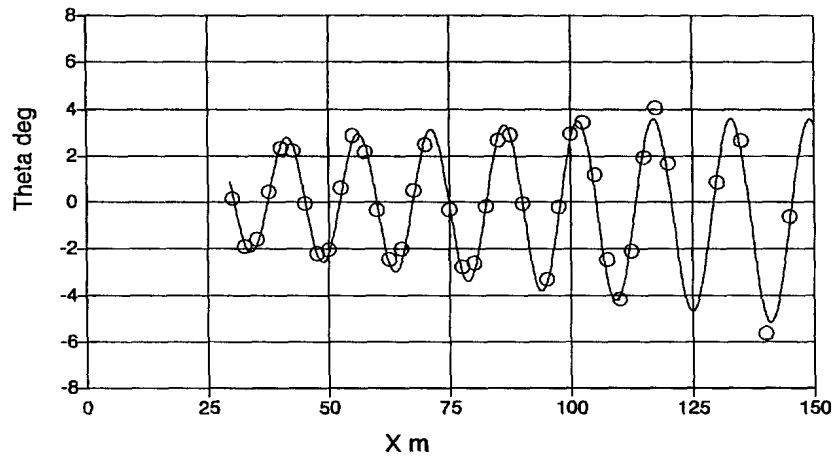
A981001

A981001

A981001
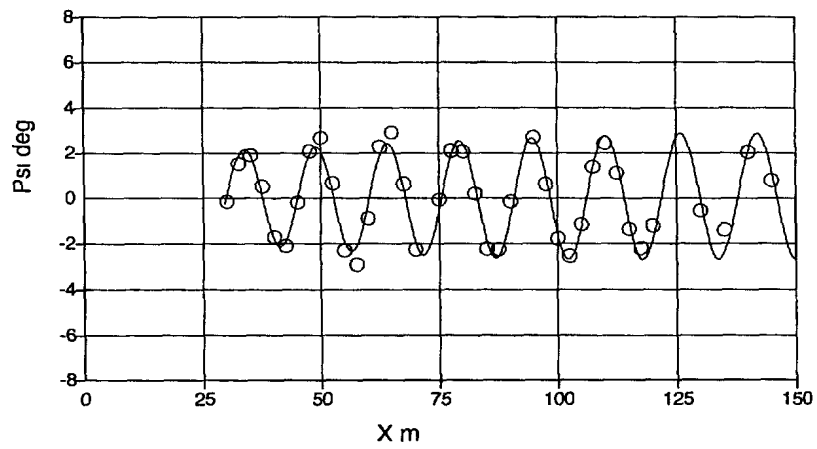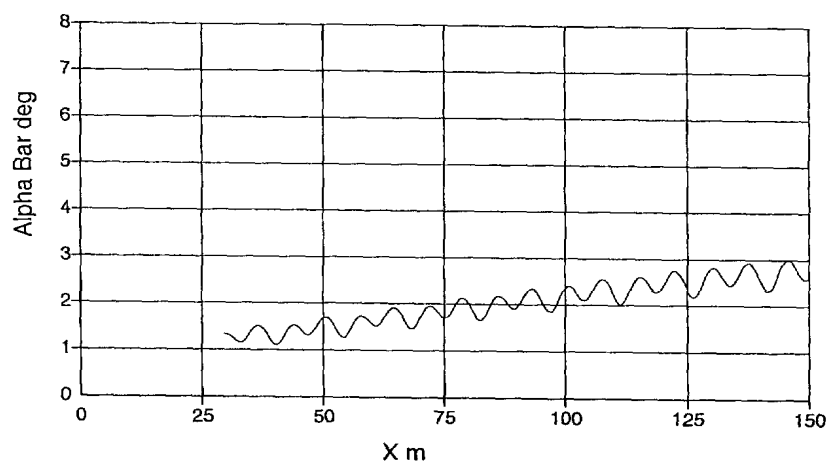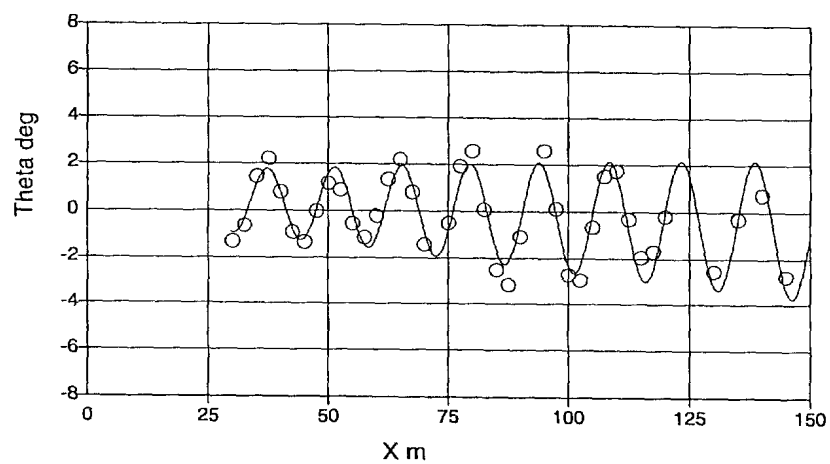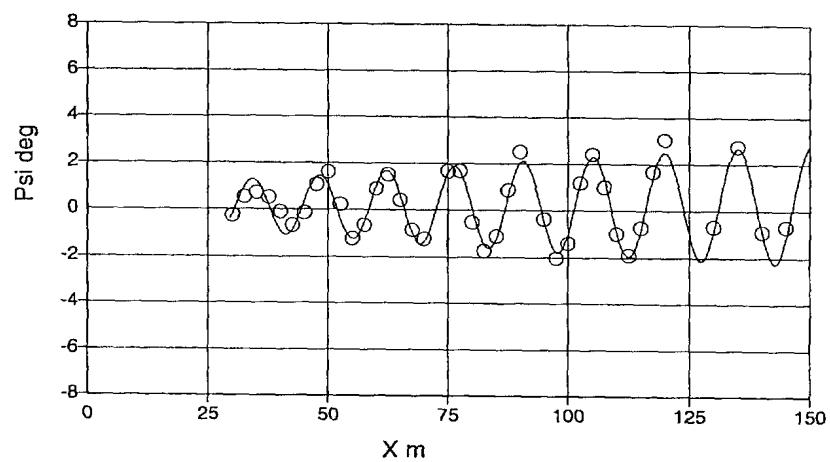
A981002

A981002
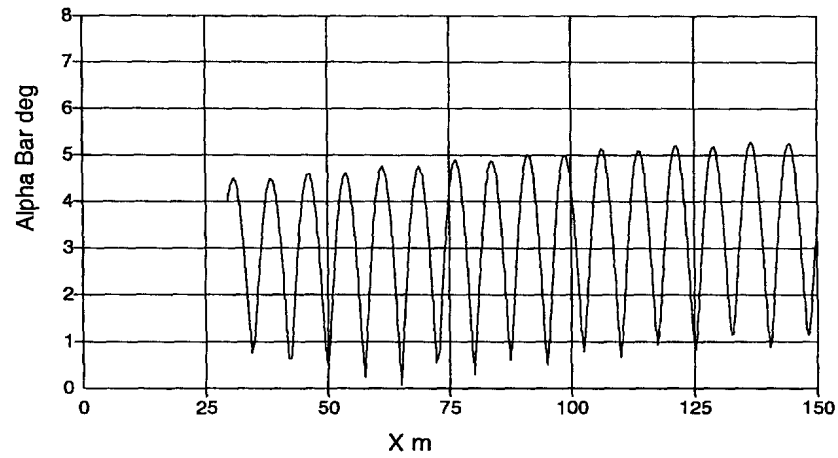
A981002
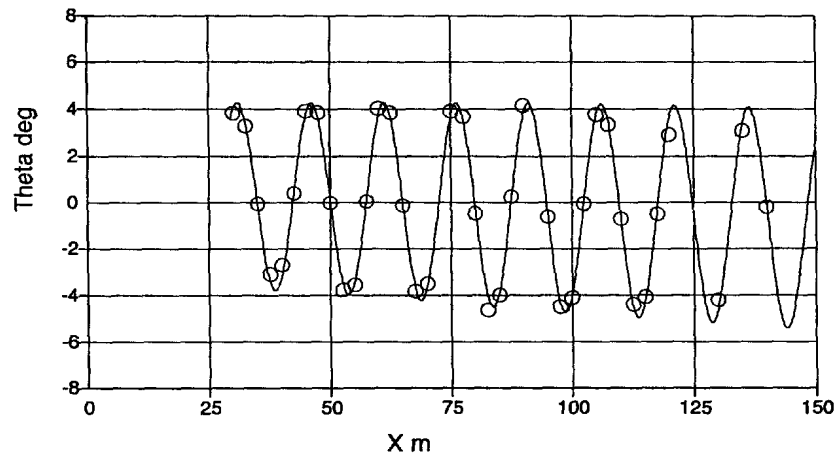
A981003

A981003

A981003
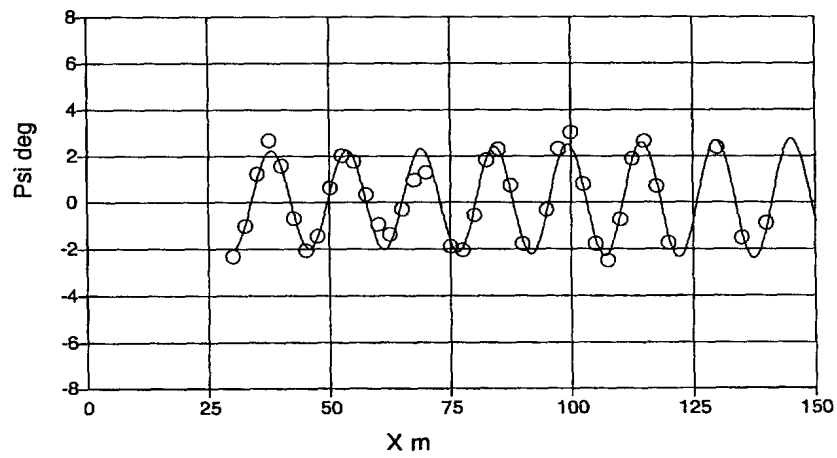
UNCLASSIFIED

A981004
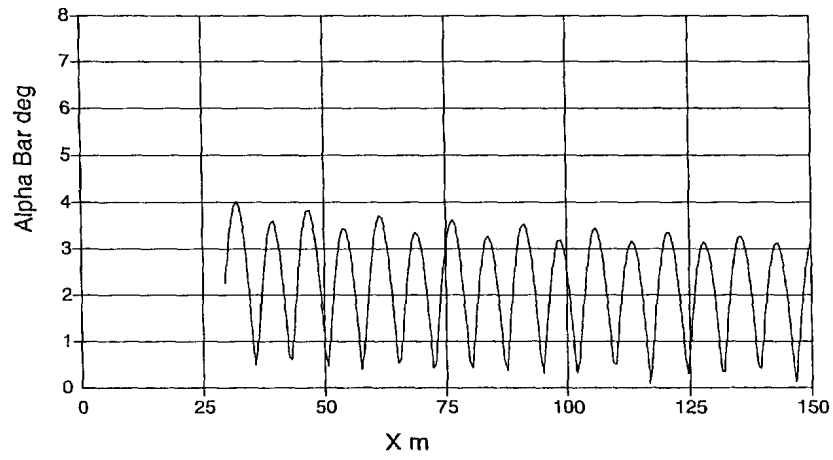
A981004
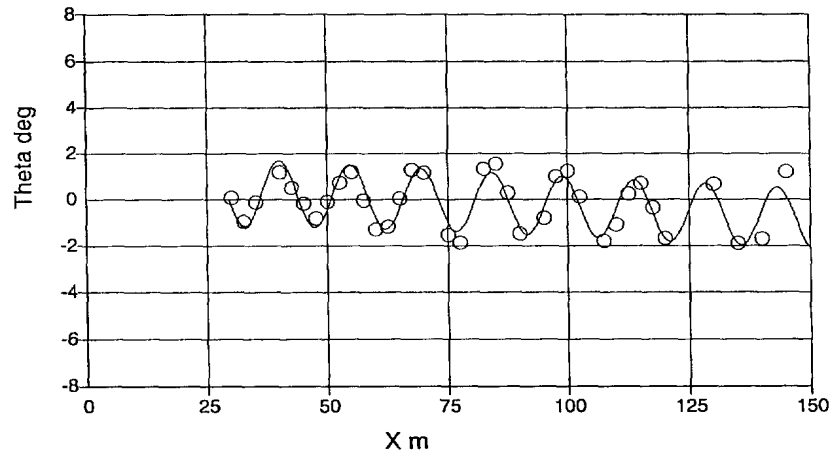
A981004
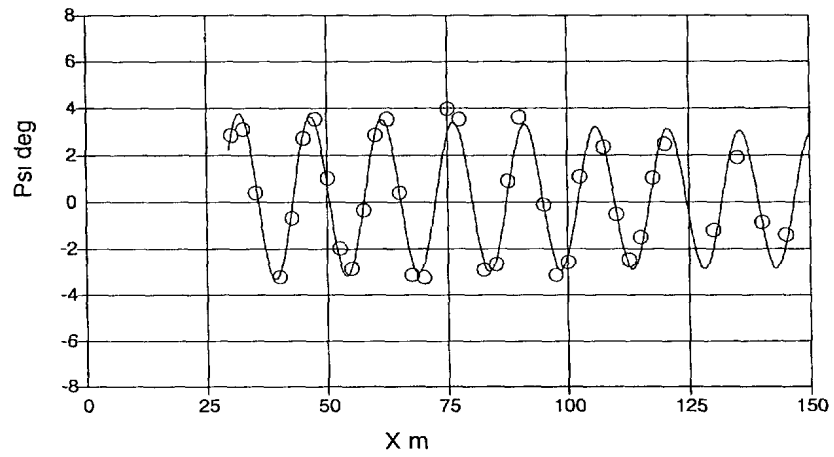
UNCLASSIFIED

A981005
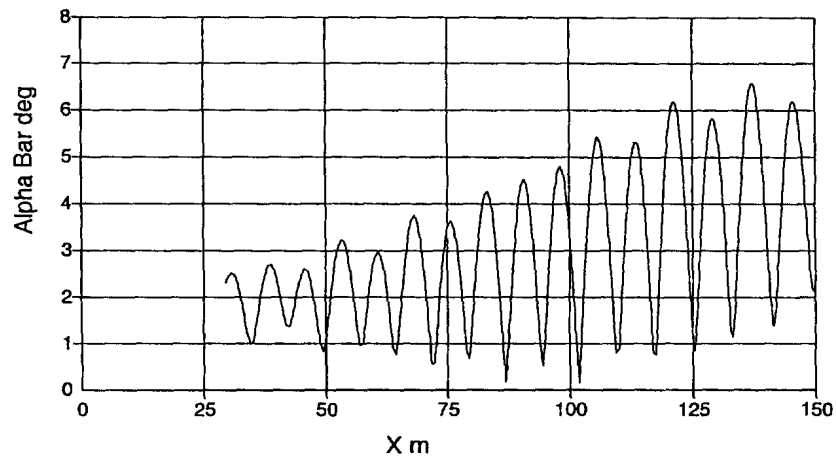
A981005
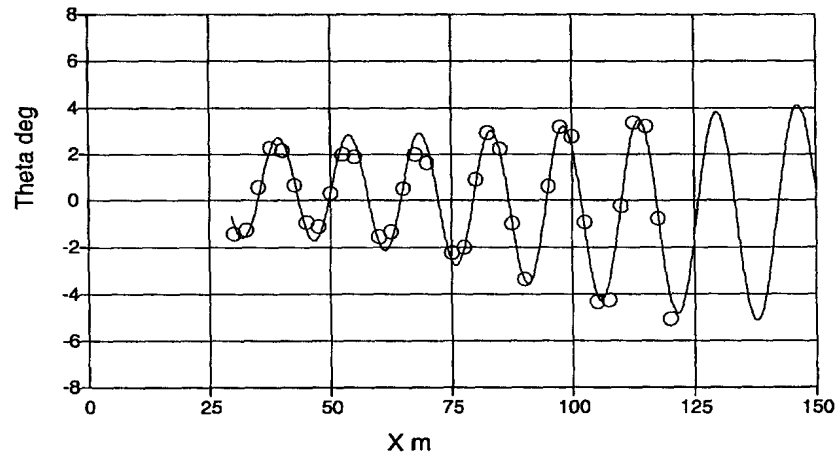
A981005
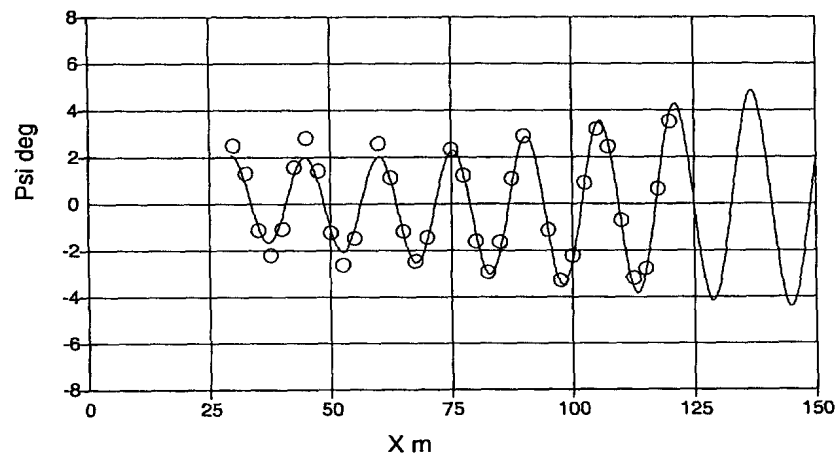
UNCLASSIFIED

A981006
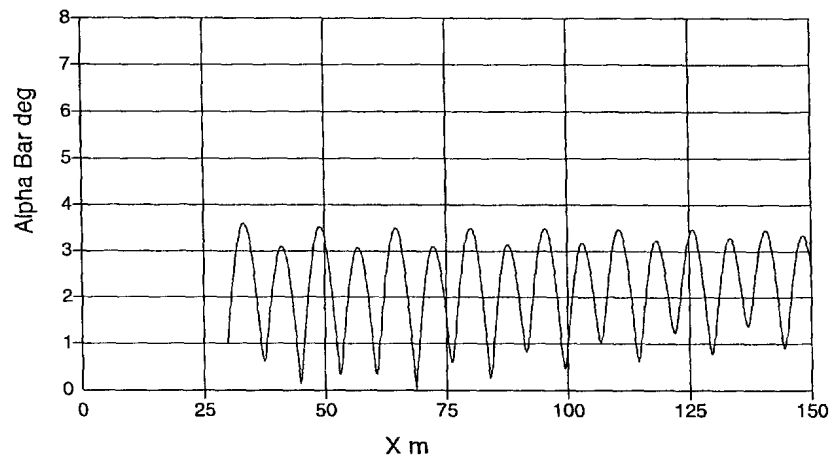
A981006
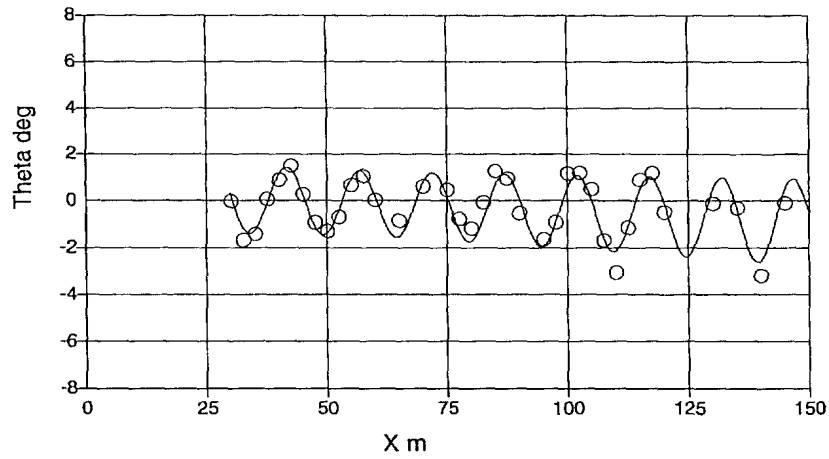
A981006
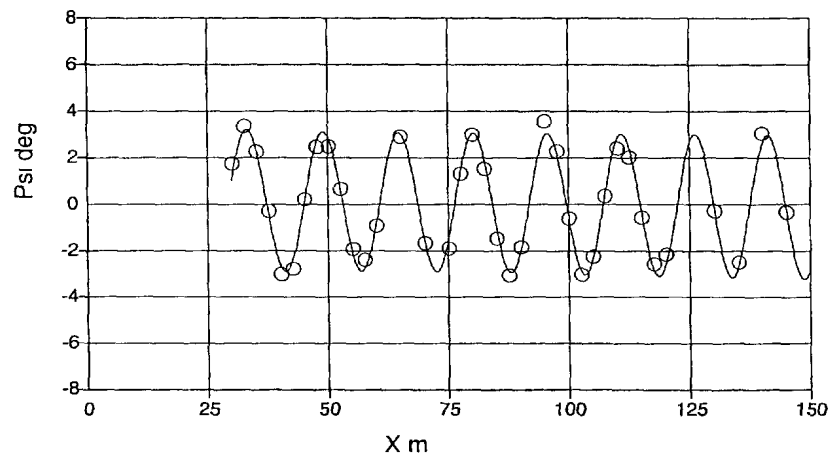
UNCLASSIFIED

A981007
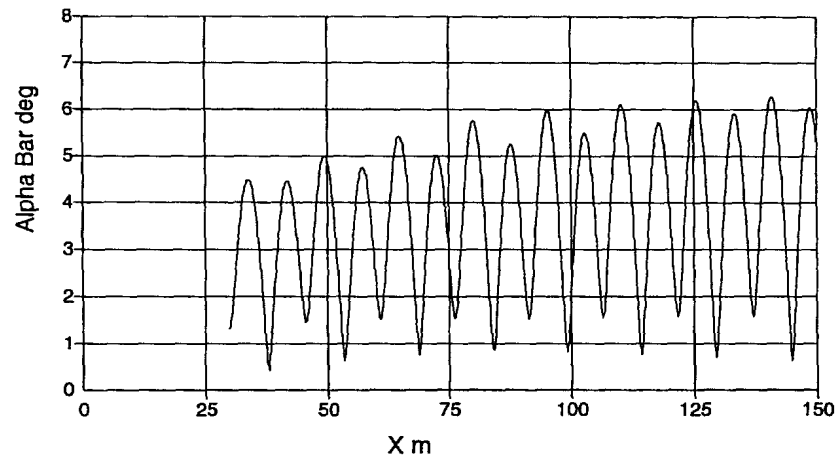
A981007
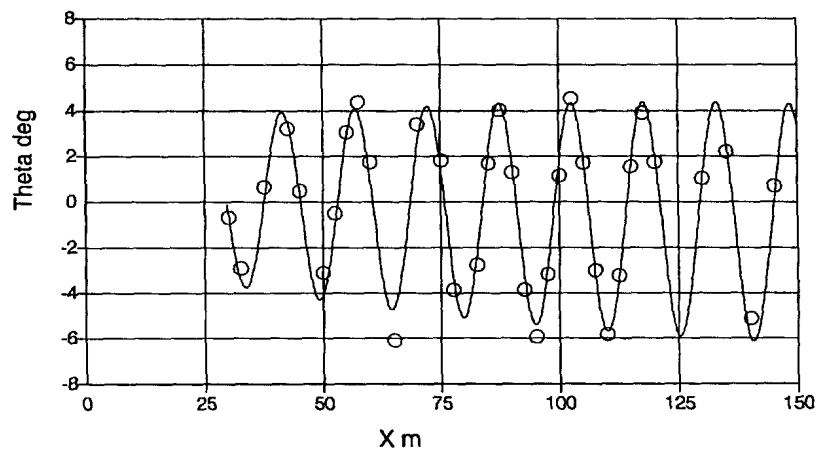
A981007
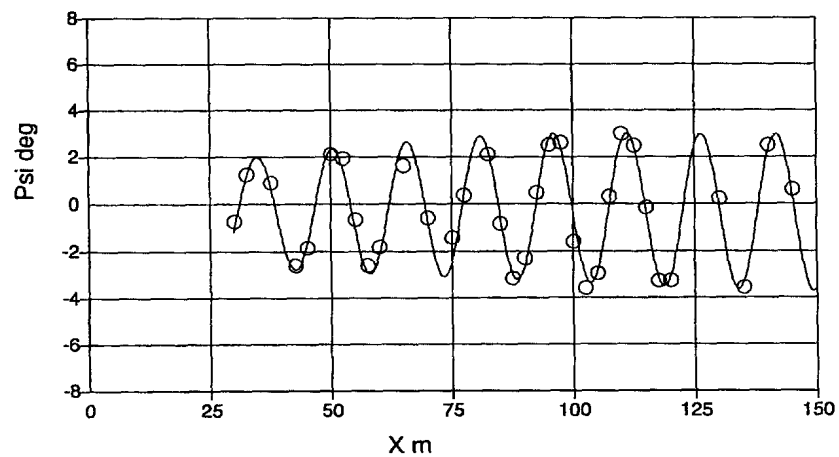
UNCLASSIFIED

A981008
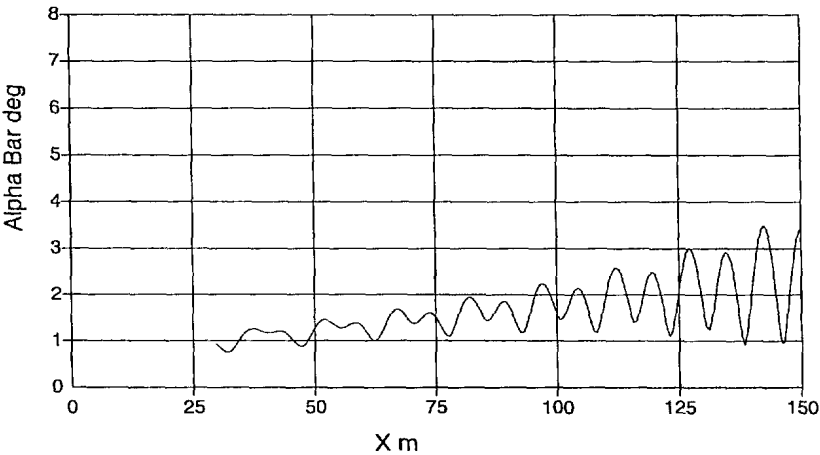
A981008
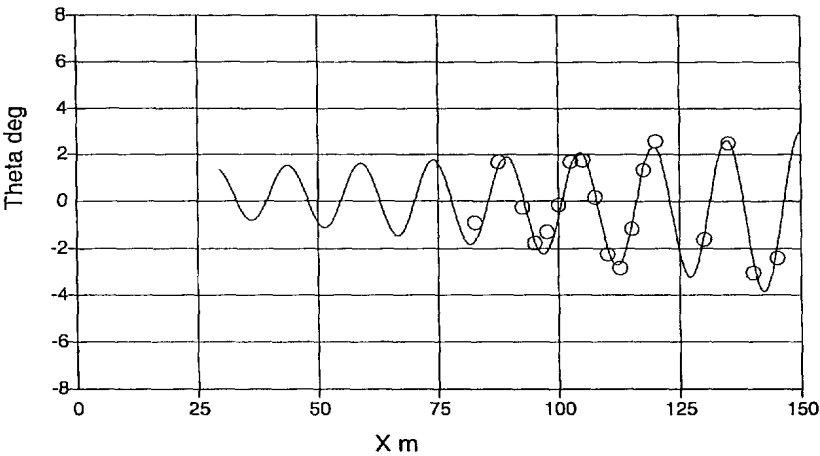
A981008
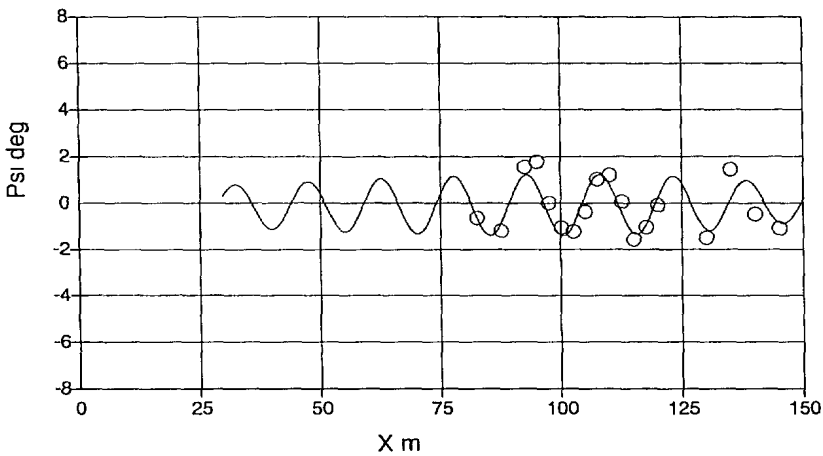
UNCLASSIFIED

A981009
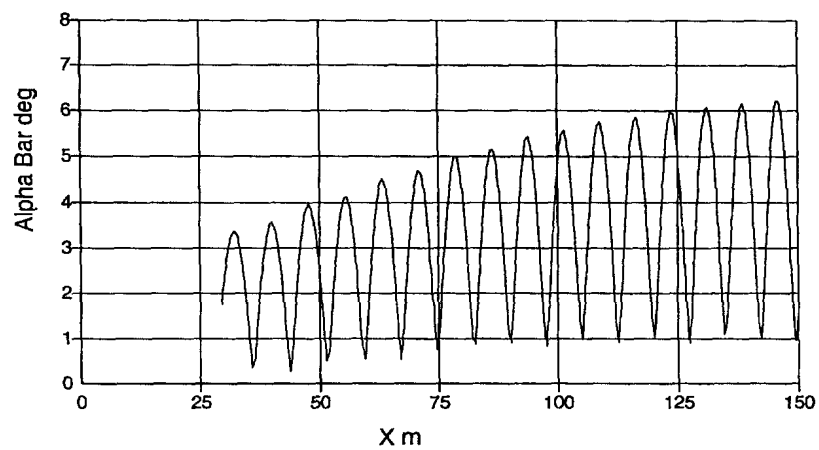
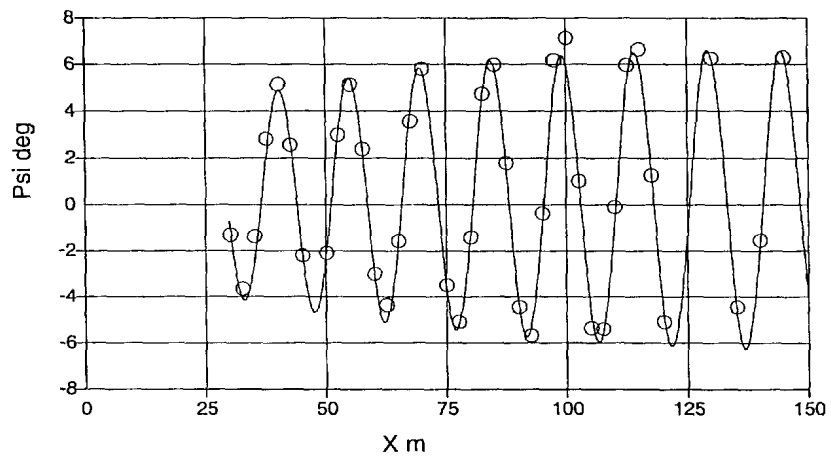
A981009
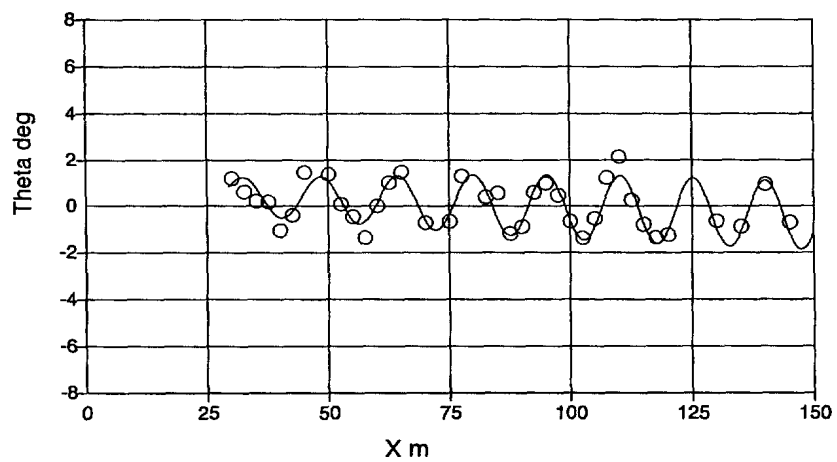
A981009
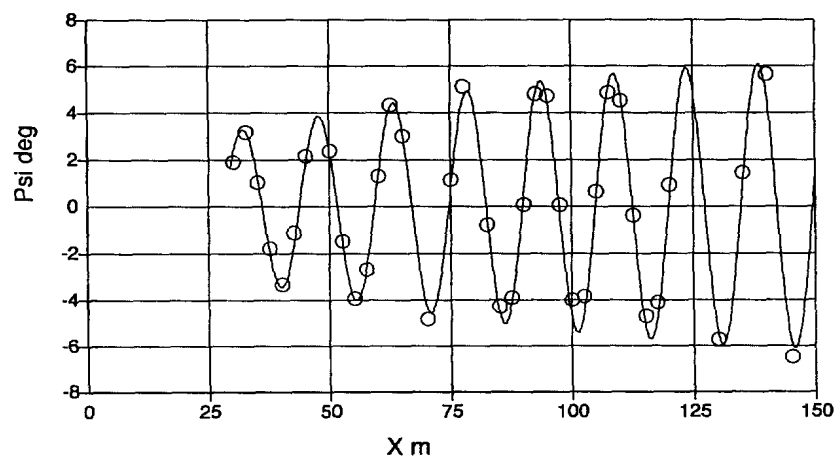
UNCLASSIFIED
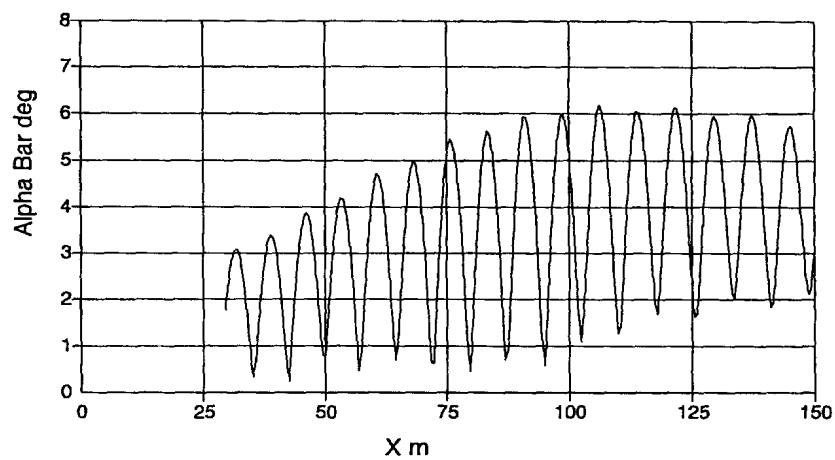
A981010
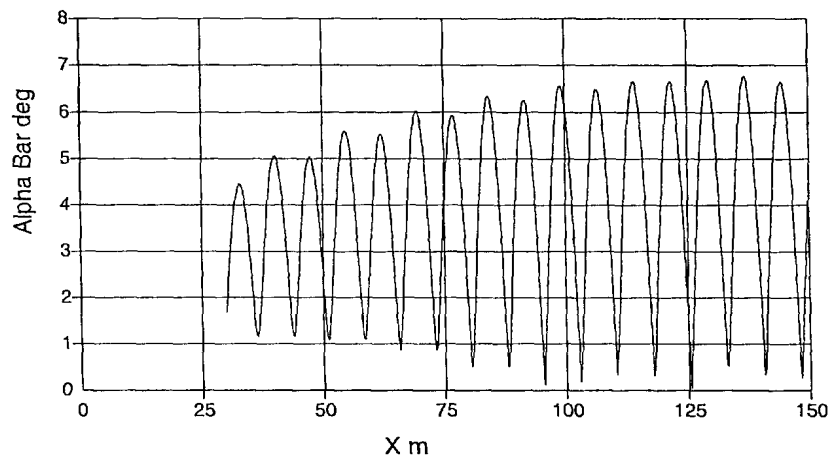
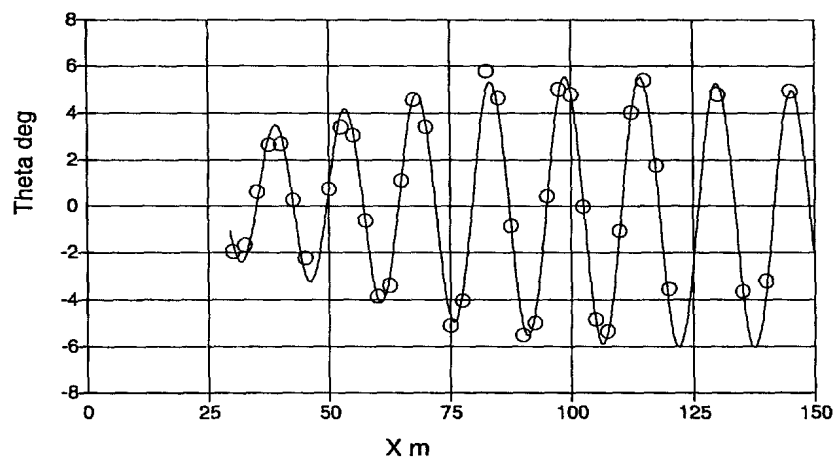
A981010
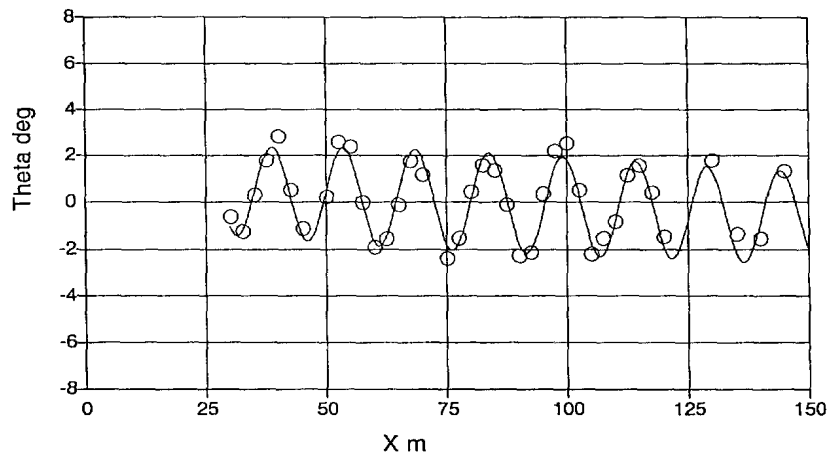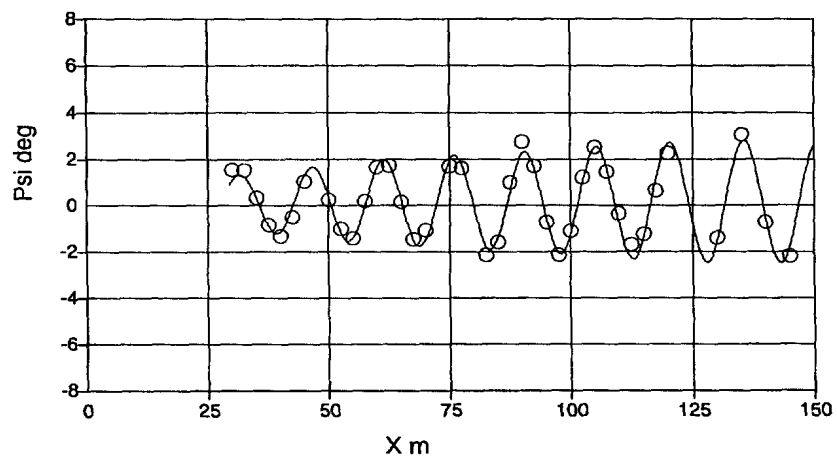

A981010

UNCLASSIFIED

A981011

A981011

A981011

UNCLASSIFIED

INTERNAL DISTRIBUTION

DREV TR 2000-229

1 – Director General

6 – Document Library

1 –A. Dupuis (author)

1 – F. Lesage

1 – É. Fournier

1 – A. Jeffrey

1 – G. Dumas

1 – R. Delagrave

1 –M. Lauzon

1 – P. Harris

1 – Maj. Côté

1 – L. Audet

1 – P. Gosselin

1 – M. Boivin

1 –D. Sanschagrin

UNCLASSIFIED

EXTERNAL DISTRIBUTION

DREV TR 2000-229

1 – DRDKIM

1 – DRDKIM (unbound copy)

1 – DRDC

1 – DSAL

1 – DLR

1 – DAR 5

1 – DNR

1 – DSAA

1 – DSAM

1 – DAEPM (FT) 3

1 – DTA

1 – DTA 3-4

1 – DAPM (ES) 4-3

2 – DRES

1 – CEEM - V

1 – AETE

1 – WSM der Mirabel/SE 6

EXTERNAL DISTRIBUTION (Continued)

DREV TR 2000-229

1 – Mr. N. Stathopoulos
    Dept. 775
    Bombardier Aerospace
    1800 Marcel Laurin Blvd
    St-Laurent, QC
    H4R 1K2

1- Mr. N. Tang
    High Speed Aerodynamic Laboratory
    Institute for Aerospace Research
    National Research Council Canada
    Montreal Road
    Ottawa, Ontario
    K1A 0R6

1-Wayne Hathaway (author)
    Arrow Tech Associates
    1233 Shelburne Road
    Suite D-8 Pierson House
    South Burlington, VT, USA, 05403

FICHE DE CONTRÔLE DU DOCUMENT

1. PROVENANCE (le nom et l'adresse) CRDV	2. COTE DE SÉCURITÉ (y compris les notices d'avertissement, s'il y a lieu) UNCLASSIFIED

3. TITRE (Indiquer la cote de sécurité au moyen de l'abréviation (S, C, R ou U) mise entre parenthèses, immédiatement après le titre.)
Aerodynmic Characteristic of the BDU-5003/B MOD 1 Bomb at Subsonic Velocities fromAeroballistic Range Free-Fligth Tests

4 AUTEURS (Nom de famille, prénom et initiales. Indiquer les grades militaires, ex.: Bleau, Maj. Louis E.)
A. Dupuis, A. Dupuis

5. DATE DE PUBLICATION DU DOCUMENT (mois et année) Juin 2000	6a. NOMBRE DE PAGES 80	6b. NOMBRE DE REFERENCES 15

7. DESCRIPTION DU DOCUMENT (La catégorie du document, par exemple rapport, note technique ou mémorandum. Indiquer les dates lorsque le rapport couvre une période définie.)
rapport

8. PARRAIN (le nom et l'adresse)
DTA NDHQ

9a. NUMÉRO DU PROJET OU DE LA SUBVENTION (Spécifier si c'est un projet ou une subvention) 3ec16	9b. NUMÉRO DE CONTRAT

10a. NUMÉRO DU DOCUMENT DE L'ORGANISME EXPÉDITEUR	10b. AUTRES NUMÉROS DU DOCUMENT N/A

11. ACCÈS AU DOCUMENT (Toutes les restrictions concernant une diffusion plus ample du document, autres que celles inhérentes à la cote de sécurité)

- ☒ Diffusion illimitée
- ☐ Diffusion limitée aux entrepreneurs des pays suivants (spécifier)
- ☐ Diffusion limitée aux entrepreneurs canadiens (avec une justification)
- ☐ Diffusion limitée aux organismes gouvernementaux (avec une justification)
- ☐ Diffusion limitée aux ministères de la Défense
- ☐ Autres (préciser)

12. ANNONCE DU DOCUMENT (Toutes les restrictions à l'annonce bibliographique de ce document Cela correspond, en principe, aux données d'accès au document (11). Lorsqu'une diffusion supplémentaire (à d'autres organismes que ceux précisés à la case 11) est possible, on pourra élargir le cercle de diffusion de l'annonce.)
illimit/e

dcd03f

SANS CLASSIFICATION

COTE DE LA SÉCURITÉ DE LA FORMULE
(plus haut niveau du titre, du résumé ou des mots-clefs)

13. SOMMAIRE (Un résume clair et concis du document. Les renseignements peuvent aussi figurer ailleurs dans le document Il est souhaitable que le sommaire des documents classifies soit non classifie Il faut inscrire au commencement de chaque paragraphe du sommaire la cote de sécurité applicable aux renseignements qui s'y trouvent, à moins que le document lui-même soit non classifie Se servir des lettres suivantes· (S), (C), (R) ou (U) Il n'est pas nécessaire de fournir ici des sommaires dans les deux langues officielles à moins que le document soit bilingue)

Free-flight tests were conducted in the Defence Research Establishment Valcartier (DREV) aeroballistic range on a full scale MPB-HD (BDU-5003/B MOD 1) bomb at subsonic velocities All the main aerodynamic coefficients and dynamic stability derivatives were very well determined using the six-degree-of-freedom single- and multiple-fit data reduction techniques The free-flight data shows that this bomb is dynamically unstable at low angles of attack The second order pitch damping coefficient, the yaw axial force term as well as side moments were also reduced Wind tunnel, Open Jet Facility experimental results and full-scale aircraft free-flight trials were compared with the aeroballistic ones

14. MOTS-CLÉS, DESCRIPTEURS OU RENSEIGNEMENTS SPÉCIAUX (Expressions ou mots significatifs du point de vue technique, qui caractérisent un document et peuvent aider à le cataloguer Il faut choisir des termes qui n'exigent pas de cote de sécurité Des renseignements tels que le modèle de l'équipement, la marque de fabrique, le nom de code du projet militaire, la situation géographique, peuvent servir de mots-clés Si possible, on doit choisir des mots-clés d'un thésaurus, par exemple le "Thesaurus of Engineering and Scientific Terms (TESTS)" Nommer ce thésaurus. Si l'on ne peut pas trouver de termes non classifiés, il faut indiquer la classification de chaque terme comme on le fait avec le titre)

FREE-FLIGHT TESTS
MODUDLAR PRACTICE BOMB - HIGH DRAG
AERODYNAMIC COEFFICIENTS
6DOF
MLM METHODOLOGY
AEROBALLISTIC RANGE TESTS
LINEAR THEORY
BOMBS
GUN LAUNCHED
SUBSONIC
FINNED PROJECTILE
DYNANMV INSTABILITY
FLIGHT DYNAMICS
STABILITY
NONLINEAR AERODYNAMICS
HIGH DRAG DEVICES

#515888

CA011310

SANS CLASSIFICATION

COTE DE SÉCURITÉ DE LA FORMULE
(plus haut niveau du titre, du resumé ou des mots-clefs)

dcd03f